ADDIS ABABA UNIVERSITY
School of Graduate Studies
Department of Chemistry

Graduate project
(Chem-774)

Electrocatalytic reduction of oxygen at poly(4-amino-3-hydroxynaphtalene sulfonic acid), poly(2aminobenzoic acid) and poly(8-aminonaphtalene -2-sulfonic acid) -modified glassy carbon electrodes

By: Teklewold Getachew

Advisor: Shimelis Admassie (PhD)

In Partial Fulfillment of the Requirements for Master of Science Degree in Chemistry

---

July, 2009

ADDIS ABABA UNIVERSITY
School of Graduate Studies
Department of Chemistry

Graduate project
(Chem-774)

Electrocatalytic reduction of oxygen at poly(4-amino-3-hydroxynaphtalene sulfonic acid), poly(2aminobenzoic acid) and poly(8-aminonaphtalene -2-sulfonic acid) -modified glassy carbon electrodes

Approved by the Examining Board: **Signature**

Dr. Shimelis Admassie _____

Advisor

Prof. Theodros Solomon _____

Examiner

Dr. Teketel Yohannes _____

Examiner

Declaration

I the undersigned confirm that the results reported in this work were obtained by research carried out by me under the supervision of my Advisor in the Faculty of Science, Department of Chemistry, Addis Ababa University.

Name: Teklewold Getachew

Signature: _____

This project work has been submitted for examination with my approval as university advisor.

Advisor — signature

Dr. Shimelis Admassie — _____

Place and date of submission: School of Graduate Studies
Addis Ababa University
July, 2009

ACKNOWLEDGEMENTS

I thank the almighty God who give the strength and helped me in all of my work.

It is a great pleasure to acknowledge my advisor, Dr. Shimelis Admassie for his continuous guidance, encouragement, creating conducive environment and support with materials during the course of the project.

My deep gratitude goes to Mekdes Mohammed, Dejene Demisse, Misrak Tulu and kebebush Tulu for their material and moral support in all of my study in the postgraduate program.

I am also grateful to all academic staff and technical assistance of chemistry department of A.A.U.

Table of Contents

LIST OF FIGURES

LIST OF TABLES

LIST OF ABBREVIATIONS

ORR	Oxygen reduction reaction
PEMFC	Polymer exchange membrane fuel cell
DMFC	Direct-methanol fuel cell
AFC	Alkaline fuel cell
PAFC	Phosphoric-acid fuel cell
SOFC	Solid oxide fuel cell
MCFC	Molten-carbonate fuel cell
GCE	Glassy carbon electrode
PMEs	Polymer-modified electrodes
ECPs	Electronically conducting polymers
PANI	Poly aniline
SPANI	Sulfonated polyaniline
PEDOT	Poly (3,4-ethylenedioxy thiophene)
AHNSA	4-Amino-3-hydroxynaphtalene sulfonic acid
ABA	2-aminobenzoic acid
ANSA	8-Aminonaphtalene -2-sulfonic acid
CV	Cyclic voltammetry
RDV	Rotating disk Voltammetry
RDE	Rotating disk electrode
RRDE	Rotating ring disk electrode

Abstract

The electrochemical behavior and the electrocatalytic activity of polymer modified glassy carbon electrodes for oxygen reduction reaction (ORR) were examined using cyclic and rotating disk voltammetric techniques. Glassy carbon electrodes were modified by electropolymerization of 4-amino-3-hydroxynaphtalene sulfonic acid (AHNSA), 2-aminobenzoic acid (ABA) and 8-aminonaphtalene-2-sulfonic acid (ANSA). Use of a rotating disk electrode allowed to separate the different contributions in the overall reaction: diffusion of molecular oxygen in the electrolyte solution (0.5M H_2SO_4), diffusion inside the film, adsorption process and electron transfer. Koutecky- Levich analysis made possible to evaluate the kinetic parameters (total number of exchanged electron, limiting current density, Tafel slope and exchange current density). The electrocatalytic behavior of 4-amino-3-hydroxynaphtalene sulfonic acid (AHNSA) , 2-aminobenzoic acid (ABA) and 8-aminonaphtalene-2-sulfonic acid (ANSA) modified glassy carbon electrodes were compared based on both the exchange current density (i^o) and the overpotential values at a common current density.

Keywods: Electrocatalysis, Electropolymerization, ORR, Overpotential, Tafel slope

1. INTRODUCTION

Oxygen electrochemistry, particularly the reaction mechanism of oxygen reduction and the role of electrocatalysis in oxygen reduction reaction has great importance since it has been the most important issue in the development of fuel cells, metal air batteries, industrial electrocatalytic process and electro-organic reactions [1].

Oxygen reduction reaction (ORR) is challenging for electrochemist because the reaction is sluggish and proceeds through several intermediates. Thus, ORR requires the most effective catalyst. The most familiar metal catalyst is platinum. However, the cost of platinum is very high and its supply is limited. Therefore, improvement of ORR catalyst to increase catalytic activity is a very important subject. Numerous efforts have been paid to the search for cheaper materials with excellent electrocatalytic activity towards ORR to replace the costly metal (Pt) based electrocatalyst and develop new and better electrocatalysts.

ORR occurs in various electrochemical energy conversion processes and electrocatalysis of the dioxygen reduction continuous to command a great deal of interest in modern electrochemistry owing to its technological importance in electrochemical devices. However, the current research lies in the utilization of modified electrode. Therfore, the catalytic oxygen reduction reaction is the most important electrochemical reaction in the practical, economical and theoretical point of view [2-4]

1.1 Reaction path ways for ORR [3-6]

Oxygen reduction reaction involves a number of elementary steps and various reaction intermediates. The reaction proceeds by either a four electron path ways, where the final product is water or by a two electron path way yielding hydrogen per oxide depending on the electrode materials as well as on the reaction conditions such as solution pH, electrode material and electrode potential.

If the oxygen reduction reaction proceeds through the complete four electron process with out peroxide like intermediate, it is called the direct pathway.

$$O_2 + 4\,H^+ + 4e^- \rightarrow 2\,H_2O \quad E^o = 1.229V \text{ Vs NHE (acidic media)} \qquad (1)$$

$$O_2 + H_2O + 4e^- \rightarrow 4\,OH^- \quad E^0 = 0.401V \text{ (alkaline media)} \qquad (2)$$

If the oxygen reduction proceeds entirely through the peroxide route, it is called the series path way.

$$O_2 + 2\,H^+ + 2e^- \rightarrow H_2O_2 \quad E^o = 0.67\ V \text{ Vs NHE (Acidic media)} \qquad (3)$$

This occurs on less active surface that supports a two electron reduction.

Peroxide can undergo further reduction or decomposition

$$H_2O_2 + 2H^+ + 2e^- \rightarrow 2\,H_2O \quad E^o = 1.77\ V \qquad (4)$$

$$2\,H_2O_2 \rightarrow 2\,H_2O + O_2 \qquad (5)$$

In alkaline media

$$O_2 + H_2O + 2e^- \rightarrow HO_2^- + OH^- \quad E^o = -0.065\ V \qquad (6)$$

The reaction is followed by further two electron reduction or by decomposition

$$HO_2^- + H_2O + 2e^- \rightarrow 3\,OH^- \quad E^o = 0.867\ V, \qquad (7)$$

$$2HO_2^- \rightarrow 2\,OH^- + O_2 \qquad (8)$$

If the reaction proceeds through both the direct and series pathways it is said to be parallel pathway. This is the pathway for most oxygen reduction catalysts.

The electronic and morphological properties of the electrode surface will determine the extent to which the mechanism proceeds through direct, series or parallel pathway. Therefore, focus on the surface physics of oxygen electrocatalysts aimed at an improved understanding of the structure and composition of the electrode surface in relation to its activity for ORR becomes an important issue.

Oxygen adsorption is a complex processes in which there are no reliable information on the site and configuration of oxygen adsorption on electrode surface. However, three distinct models have been proposed for the oxygen reduction reaction on transition metal

electrocatalysts in acid media and are referred as the Griffiths, Pauling and Yeager (bridge) models.

Griffiths model

In this model O_2 interacts with two bonds with a single substrate atom.

The bond formed mainly between π- orbitals of O_2 and empty d_z^2 orbitals on the metal surface atom with a π back bond from the partially filled d_{xy} or d_{yz} orbitals of the metal to the antibonding π* orbitals of O_2.

Pauling model

In this model, end on adsorption through a single bond in a σ type bond with a σ orbitals of O_2 donates electron density to an acceptor d_z^2 orbitals on the metals. The Pauling adsorption primarily leads to the peroxide route depending on which oxygen atom the second proton attacks.

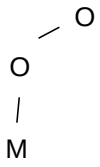

Bridge (Yeager) model

This model involves the formation of a bridge bonded structure formed by the interaction between the oxygen SP^2 π orbitals and the partially filled d_{xy} or d_{yz} orbitals of the two surface atoms principally for the reaction on platinum metals.

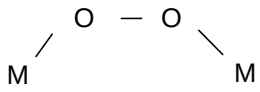

Yeager adsorption is typically followed by oxygen bond dissociation, where the oxygen reduction proceeds exclusively through the direct route. Four electron reduction reactions takes place in the case of Griffits and bridge models, while parallel two and four electrons reduction simultaneously take place in the pauling model.

Reaction pathways are analyzed based on data obtained by a rotating disk ring technique that enables the quantitative determination of some the reaction intermediates. Several reaction schemes were proposed for analyzing the disk ring data and calculating the rate of various reaction steps. One of the difficulties in determining the correct scheme is that the number of experimentally obtained quantities from the ring disk measurement is usually not sufficient to determine all the parameters on the model. Consequently, simple scheme (Fig.1) Which has too fewer rate constants is used.

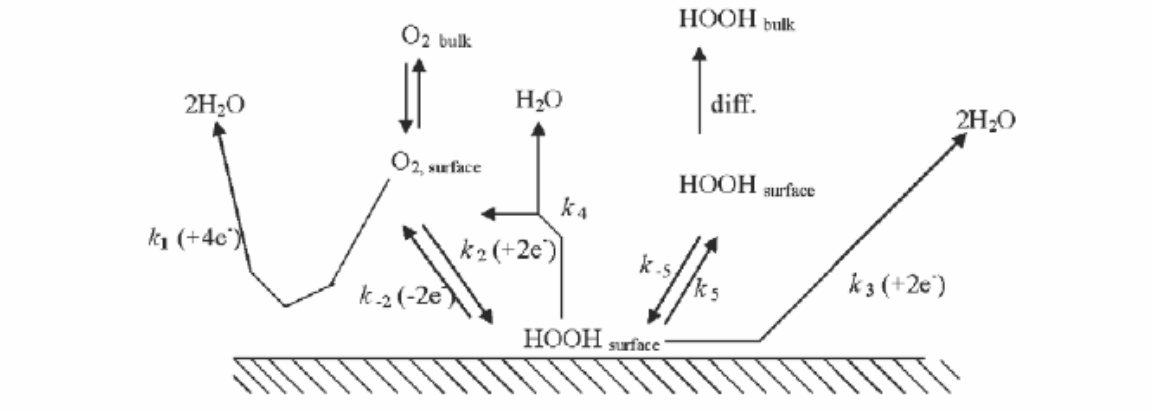

Fig. 1 Schematic presentation of ORR pathway suggested by Wroblowa

1. 2 Electrocatalysis for oxygen reduction on Noble metal based Electrodes

Oxygen reduction takes place at high positive potentials. At such potentials most of the metals will dissolve and only noble metals and some of their alloys offer possibilities among metallic systems. The most familiar oxygen reduction catalysts are based on noble metals, particularly platinum.

At present, only platinum is viewed as a viable metal catalyst for ORR. However, the cost of Pt is too high for world wide implementation of fuel cell. Aiming to increase the

catalytic activity of oxygen reduction and to lower the cost of catalysts various Pt-based alloys are under study. Improvement in ORR activity have been commonly associated with nanophase multimetallic alloys, such as Pt - Co, Pt –Ni, Pt- Cr & Pt- Fe supported on carbon electrode.

For pure platinum supported on carbon, it is well established that the mass activity (current based on the total mass platinum) is at a maximum when its particle size is optimized at around 3.5 nm [6 -7]**.**

The improvement in the ORR electrocatalyst on Pt alloy catalyst has been explained by several factors, such as electronic and structural effects [8]. Jalan and Taylor [9] investigate Pt-based alloy catalysts for the ORR and suggested that the enhanced electrocatalytic activity is due to the shortening of the Pt-Pt mean interatomic distance (geometric factor). Mukerjee and Srinivasan [10] and Min et al [11] reported that the enhanced electrocatalytic activity is due to an increase in the Pt-d band valancy (electronic factor). Paffet et al. [12] reported that the enhanced electrocatalytic activity is ascribed to the surface roughening.

1. 2.1 ORR on platinum, Gold and silver in acidic solution [5]

For platinum and platinum group metals no, or very little, hydrogen peroxide is generated. It occurs by the parallel mechanism with predominantly direct electron reduction.

Oxygen reduction on gold in acidic solution is a very slow process and strongly depends on structure. ORR on gold involves a two electron reaction, with hydrogen peroxide as the reaction product. Gold appears to be the unique metals that in addition to a two electron reduction supports a four electron reduction.

Oxygen reduction reaction on silver is a four electron reduction. The difference between the activities of gold and silver surface for O_2 reduction is a consequence of the difference

electronic structure of the two metals. Gold is very inactive for adsorption of O_2 from the gas phase. Molecular orbital consideration shows that end-on adsorption of O_2 is expected on gold, while for silver, bridge adsorption should be more favorable.

1. 2. 2 ORR on platinum and Gold in alkaline solution

ORR in alkaline electrolytes has been of great interest due to its known importance for alkaline fuel cells. The two electron reduction mechanism with the formation of hydrogen peroxide ion (HO_2^-) is widely adopted [13].

In alkaline solution the parallel mechanism is operative for oxygen reduction on platinum. The extent of electrocatalysis in alkaline solution appears to be smaller than in acidic solution.

Oxygen reduction on gold in alkaline solution is structure sensitive reaction. The four-electron reduction is observed for a limited potential region for Au (100) outside this potential region, a two electron process is operative [5].

1.3 Electrocatalysis for oxygen reduction on non noble metal based Electrodes

Oxygen reduction on non noble metals attracted considerable attention recently, primarily because of its role in corrosion [5].

1.3.1 Transition metal oxides [6]

Transition metal oxides possess appreciable chemical and /or electrocatalytic activity, which make them versatile materials for chemical and electrochemical reactions because of their abilities to switch between different valencies. For the same reasons, these oxides exhibit remarkable stabilities toward chemical and electrochemical attack in appropriate conditions. In general, oxide cathodes are of two types:

1) A porous, metallic oxide or a metallic oxide dispersed on or with carbon to form a porous metallic matrix. The oxide is catalytically active for ORR in the case of all electrochemical devices. In this case, ORR occurs at a catalyst/electrolyte/air three phase linear interphase.

2) A mixed electrode/ oxide ion conductor that catalyzes the ORR is coated as a film on a solid oxide ion electrolyte. In this case ORR occurs over the entire surface of the oxide film.

1. 3. 2 Transition metal chalcogenides [14]

An interesting electrocatalyst for O_2 reduction has been obtained by utilizing metal cluster Chevrel compounds. These materials are of interest firstly because of the increased delocalization of electrons in cluster and because of the availability of a reservoir of charges for the multi-electron charge transfer.

The Chevrel compounds are molybdenum chalcogenides with general formula $M_xMo_6X_8$,where M represents a vacancy, a rare earth element, a transition, or a main group metallic element, and X is S, Se, or Te.

Some of these materials selectively reduce oxygen to water even in the presence of methanol by the direct transfer of four electrons under acidic conditions, which makes them as promising cathode materials for electrochemical devices such as Polymer exchange membrane fuel cell (PEMFC) and Direct-methanol fuel cell (DMFC).

Ternary chalcogenides of the formula $M_xMo_6X_8$ (M= Cu, Ag, Ni, Fe, Pb and X= S, Se, or Te) have been the synthesized by Chevrel in 1971 and therefore are often referred to as chevrel compounds.

1.3. 3 Transition metal macrocyclic complex

Macrocyclic derivatives of transition metals constitute a unique class of electrocatalyst for ORR. Catalytic activity for oxygen reduction reaction is found only with a macroligand, which has a cyclic conjugation of ' π' electrons. They function in both acid and alkaline solutions.

The activity of these systems can be explained by the following three concepts:

- Application of MO theory to these systems has shown that the highest interaction of O_2 with the central metal ion (e.g Fe(II) & (Co(II)), the more the O-O bond is weakened and the more easily the molecule is reduced [5 & 15].

- If the electronic level of the electrode and reactant lie too far apart, the transition of electrons is improbable. The catalyst should then acts as a mediator supplying intermediates levels thus increasing the probability of electron transport. This approach has been proposed by Ulstrup [16].

- The third concept is developed by Beck [17]. In this concept the redox potential of the central atom ion is crucial. The interaction of O_2 molecule with metal center in the macrocycle causes a partial electron transfer from the frontier orbitals of the metal to the frontier orbital of the O_2.The precursor or adduct formed undergoes further reduction to give intermediate species like peroxide which can be the product or decomposed/reduced further to give water. The dependency of the kinetics of the reaction on the nature of the central metal ion indicates that the metal is the site where the electrocatalytic process occurs. Elements of the catalyst take part easily in a redox reaction, and thereafter the reduced material is chemically oxidized by oxygen.

The crucial steps in the catalytic cycle are given as follows:

$$M(III)OH + e^- \rightarrow M(II) + OH^- \quad (9)$$

$$M(II) + O_2 \rightarrow M(III) + O_2^-(ads) \quad (10)$$

$$M(III) + O_2^-(ads) + e^- \rightarrow \text{intermediates} \quad (11)$$

The last step is the rate determining and leads to the breaking of the O-O bond. According to this redox mechanism, the redox potential of M(III) / M(II) must be located within an appropriate, rather narrow window of potential values to obtain maximum activity [15].

1.4 Oxygen reduction reaction in fuel cells [15, 18]

Energy consumption that relay on the combustion of fossil fuels is forecast to have a severe future impact on the world economy and ecology. Hence, the development of alternative cheap, clean energy devices is important and urgent. Electrochemistry comes to the forefront of near future technology in the conversion of chemical energy to electricity and in the storage of electricity. The energy change in chemical reaction can be converted directly to electricity.

The electrochemical devices such as batteries, capacitors and fuel cells are among the most promising choices. Capacitors show high power density, but the energy density is low. Batteries supply large amount of energy, but the continuous operation time is limited by the active materials stored. The fuel cells, however, provide comparable power to batteries and generate electricity continuously because of the continuous active materials (fuel) supply. The fuel cells produce moderate power but high energy.

The fuel cell systems are simple and few. The product of the cell is generally water, which makes them “zero emission”. These advantages cause the fuel cell one of the most promising candidates for energy conversion.

The electrochemical reduction of molecular oxygen is important especially for devices such as metal air batteries (e.g Zinc–air battery) and fuel cells. Therefore, the development of efficient catalysts and electrodes requires great focuses in order to improve the inefficiency specially in fuel cells. Oxygen reduction reaction is an important reaction, because it is the greatest sources of inefficiency in fuel cells.

1.4.1. History of fuel cell technology and the main classification

Although the discovery of fuel cells is generally accredited to the English actuary Sir William Grove, it appears that Sir Humphry Davy was the first to produce electricity from chemical reaction in a cell.

Types of Fuel Cells

There are several different types of fuel cells, each using a different chemistry. Fuel cells are usually classified by their operating temperature and the type of electrolyte they use. The main types of fuel cells include:

- Polymer exchange membrane fuel cell (PEMFC)
- Direct-methanol fuel cell (DMFC)
- Alkaline fuel cell (AFC)
- Phosphoric-acid fuel cell (PAFC)
- Solid oxide fuel cell (SOFC)
- Molten-carbonate fuel cell (MCFC**)**

Polymer exchange membrane fuel cell (PEMFC / polymer electrolyte fuel cell (PEFC))

It consists of solid phase polymer membrane (typically fluorinated sulfonic acid polymer) is used as the electrolyte, which simplifies issues like sealing, assembly, storage and handling which are cumbersome for other fuel cell systems. The PEMFC typically operate at relatively low temperature (60^oC-100^oC) allowing for faster startup and immediate response to change in the demand of power.

The electrolyte of proton exchange membrane fuel cell is a solid polymer which allows protons to pass through but not electrons. With a solid and immobile electrolyte, this type of cell is inherently very simple. PEMFC is the most promising fuel cells to be commercialized for various applications.

Anode reaction:

$$2\,H_2 \rightarrow 4H^+ + 4e^- \quad (12)$$

Cathode reaction:

$$O_2 + 4H^+ + 4e^- \rightarrow 2H_2O \quad (13)$$

Net reaction:

$$2H_2 + O_2 \rightarrow 2H_2O \quad (14)$$

Direct-methanol fuel cell (DMFC)

DMFC uses the same basic cell construction as for PEMFC. It has the advantage of a liquid fuel in that is easy to store and transport. The reaction for the direct conversion of methanol has a similar voltage as for hydrogen.

Anode reaction

$$CH_3OH + H_2O \rightarrow 6H^+ + CO_2 \quad (15)$$

Cathode reaction:

$$O_2 + 4H^+ + 4e^- \rightarrow 2H_2O \quad (16)$$

Overall cell reaction

$$CH_3OH + 3/2\,O_2 \rightarrow CO_2 + 2H_2O \quad (17)$$

Alkaline fuel cell (AFC)

This is one of the oldest designs for fuel cells. It uses potassium hydroxide solution as electrolyte. The activation over voltage of cathode is less than the fuel cells with an acid electrolyte.

Anode reaction: $H_2 + 2OH^- \rightarrow 2H_2O + 2e^-$ (18)

Cathode reaction: $H_2O + ½ O_2 + 2e^- \rightarrow 2OH^-$ (19)

Cell reaction $H_2 + ½ O_2 \rightarrow H_2O$ (20)

Phosphoric-acid fuel cell (PAFC)

Phosphoric acid fuel cell is the first commercialized fuel cell. H_3PO_4 is the electrolyte and operates at ~200 ^oC. Below 150 ^oC, its conductivity is reduced, and above 220 ^oC, the phosphoric acid is too volatile and tends to decompose.

Anode reaction:

$$2H_2 \rightarrow 4H^+ + 4e^- \quad (21)$$

Cathode reaction:

$$O_2 + 4H^+ + 4e^- \rightarrow 2H_2O \quad (22)$$

Net reaction:

$$2H_2 + O_2 \rightarrow 2H_2O \quad (23)$$

Solid oxide fuel cells (SOFC)

SOFC operates at ~ 800-1000 ^oC. The electrolyte consists of solid zirconium oxide, stabilized with yitrium oxide.

Anode reaction

$H_2 + O^{-2} \rightarrow H_2O + 2e^-$ (24)

$CO + O^{2-} \rightarrow CO_2 + 2e^-$ (25)

Cathode reaction $½ O_2 + 2e- \rightarrow O^{-2}$ (26)

Molten carbonate fuel cells (MCFC)

Nickel anode and nickel oxide cathode serve as catalyst which are inexpensive compared with platinum based catalyst.The electrolyte is molten mixture of alkali metal carbonate (K_2CO_3/Li_2CO_3 in a ceramic matrix of $LiAlO_2$). It operates best at ~ 560 ^oC.

Anode reaction

$$H_2 + CO_3^{-2} \rightarrow H_2O + CO_2 + 2e^- \quad (27)$$

$$CO + CO_3^{2-} \rightarrow 2CO_2 + 2e^- \quad (28)$$

Cathode reaction

$$\tfrac{1}{2} O_2 + CO_2 + 2e^- \rightarrow CO_3^{-2} \quad (29)$$

Compared with the anode, the over potential of the cathode is high due to strong kinetic inhibition of oxygen reduction reaction. This leads to cell voltage losses. The low rate for ORR at the cathode is a limiting factor in the efficiency of fuel cells. In addition oxygen reduction can also occur through an intermediate two electrons, H_2O_2 route, which can limit the efficiency of the cell.Therfore, the most effective catalyst to enhance the efficiency of fuel cells should accelerate the kinetics of the ORR at the cathode and minimize the production of H_2O_2.

2. LITERATURE REVIEW

2.1. Electrocatalytic reaction on polymer modified Glassy Carbon electrodes

Compared to metal electrode, the glassy carbon electrode (GCE) has been widely used, which due to its low residual current over a wide potential range and has minimal propensity to show deteriorated response as a result of electrode fouling [19].

Glassy carbon is impermeable to liquids and gases, and thus porosity is not an issue. It is easily mounted, polishable, and compatible with all common solvents. These properties have led to widespread use in mechanistic electrochemistry [20].

The use of bare glassy carbon electrodes for electrochemical detection has a number of limitations, such as low sensitivity and reproducibility, slow electron transfer reaction, low stability over a wide range of solution composition, and high over potential at which the electron transfer process occurs [21]. Therefore modifying electrode surface in order to improve electrode performance is necessary. Polymer modified glassy carbon is one of the design which is effective, stable and cheap alternatives for electrocatalytic reduction of oxygen.

2.1.1. Electrocatalysis at conducting polymer electrodes

Electronically conducting polymers possess a variety of properties related to their electrochemical behavior and are therefore active materials whose properties can be altered as a function of their electrochemical potential. In ‘conjugated conducting polymers’, the redox sites are delocalized over a conjugated π system; however, ‘redox polymers’ have localized redox sites.

At conducting polymer modified electrodes the processes that should be considered during electrocatalytic conversion of solution species are a heterogeneous electron transfer between the electrode and a conducting polymer layer, and electron transfer within the polymer film. As usual, this process is accompanied by the movement of charge compensating anions and solvent molecules within the conducting polymer film, and possible conformational changes of polymer structure as well. The rate of this process is determined by many factors. Among these, electric conductivity of a polymer layer, electron self-exchange rate between the chains and/or clusters of polymer, and anion movement within polymer film seem to be of great importance. The second process is the diffusion of solution species to the reaction zone, where the electrocatalytic conversion occurs.

As compared to simple electrode reactions, this process can be more complicated in cases where the electrocatalytic conversion occurs within the polymer film. Then, the diffusion of species within the film, as well as the possible electrostatic interaction of this species with the polymer film should be taken into account. Last, a chemical heterogeneous reaction takes place between solution species and conducting polymer. As a result of these complex processes, the kinetic behavior and voltammetric responses are difficult to interpret, and a great deal of attention has been paid to consider some simplified models. Some models concerning quantitative treatment of electrocatalytic reactions and charge transfer processes within polymer films were a subject of a few reviews [22].

Suitably made polymers of acetylene, pyrrole, aniline, phenylene and thiophene have an oxidized and reduced form and the two forms have dramatically different characteristics. The reduced form is a semiconductor like many others. However, the conductance of the oxidized form that is so impressive, for its conductance may exceed 10^4 times that of the conductance of Silicon, i.e., it enters the ranges of values in which metal conduct**.** The compounds “switch on” as conducting electrodes at a certain potential as one move in the anodic direction. Each polymer has a range of potentials in which it is stable and one

must not go too far. If one advances the potential too far in the anodic direction, the polymer will undergo irreversible oxidation [23].

Electrocatalyst at a modified electrode is usually an electron transfer reaction between the electrode and some solution substrate which, when mediated by an immobilized redox couple, proceeds at a lower over potential than would otherwise occur at the bare electrode [24].

2.1. 2. Electrocatalytic oxygen reduction reaction on polymer modified Glassy Carbon electrodes

The ORR at electronically conducting polymers (ECPs) such as polyaniline (PANI), polypyrrole, Polythiophene, Poly(3-methylthiophene) and poly(3,4-ethylenedioxy thiophene) (PEDOT)-modified electrodes have been studied. Interestingly, their results suggested that electrochemical investigations of the above ECPs-modified electrodes in oxygen-saturated electrolytes indicated that existence of electrocatalytic activity towards the ORR with the exception of PEDOT [25].

Among ECPs, PANI and its derivatives have been the focus of much attention. Sulfonated polyaniline (SPAN) is of interest because of its unusual physical properties, improved processability, and potential industrial applications. The solubility of polyaniline in aqueous solutions and in most common organic solvents is greatly improved by the presence of $–SO_3^-$ groups. The environmental stability of the parent polyaniline is also further improved in SPAN. The conductivity of SPAN is independent of external protonation in a broad pH range. SPAN was found to have better thermal stability than its parent polyaniline [1]. In addition to sulfonic acid groups, carboxylic acid groups as ring substituents results in influence in the properties such as solubility, pH dependent redox activity, conductivity, thermal stability, etc. In contrast to sulfonated polyaniline, very few monomers are available for the synthesis of carboxyl acid

functionalized polyaniline. Anthracitic acid (2-aminobenzoic acid) is an important monomer and is often used for the synthesis of carboxyl acid functionalized polyaniline

The conducting polymers prepared from aromatic diamine compounds also are interesting in applications due to their multifunctional groups. The compounds having polyamine groups can react with metal ions to form a complex followed by polymerization through the removal of an electron from nitrogen of amine groups.

Electrocatalytic reduction of molecular Oxygen at Poly (1,8-diaminonaphthalene) and Poly(Co(II)-(1,8-diaminonaphthalene) modified glassy carbon electrode indicates the reaction proceed through a four electron process yielding water. The electrical conducting polymers have been receiving much attention due to their unique electrical properties and several proposed applications to practical devices [2].

2.1. 3. The structure of monomers used in the study

The monomers used in this study are carboxylic derivative of aniline Anthranilic acid (2-aminobenzoic acid), Sulfonated derivative of naphthalene 4-amino-3-hydroxynaphtalene sulfonic acid (AHNSA) and 8-aminonaphtalene-2-sulfonic acid (ANSA).

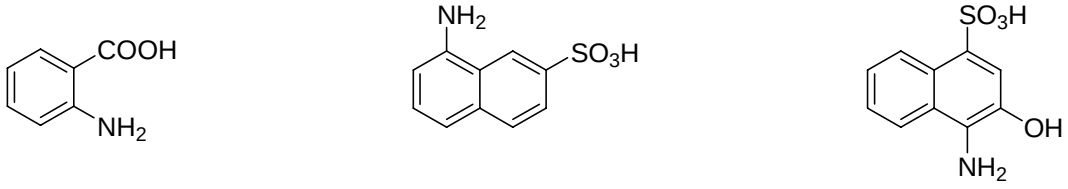

(a) (b) (c)

Fig.2 (a) Anthranilic acid (2-aminobenzoic acid) [M.wt = 137.14g/mol]
(b) 8-Aminonaphtalene -2-sulfonic acid (ANSA) [M.wt = 223.25g/mol]
(c) 4-Amino-3-hydroxynaphtalene sulfonic acid (AHNSA) [M.wt = 239.25g/mol]

3. ELECTROCHEMICAL KINETICS, TECHNIQUES AND PROCESSES

3.1. Electrode process [3, 26]

Electrode process involves all the changes and processes occurring at the electrode or in its vicinity while current flows through the cell. Electrode processes consist of the electrode reaction and the mass transport process.

The electrode reaction is an interfacial reaction that necessarily involves a charge transfer step. The rate of this type of reaction is determined by one of the consecutive steps (i.e., by the most hindered or slowest one) and the overall rate is related to the unit area of the interface.

Transport of the substance from the bulk of the electrolyte to the electrode plays an important, often rate-determining role. The electron transfer step occurs at the interface. The product of the redox reaction is transported back to the bulk. Purely chemical reactions may precede or follow these steps. Specific interactions of any species present in the electrolyte with the electrode surface leads to adsorption, which may considerably influence the overall process.

3.1.1. Transport

Three types of mass transport are important

- Diffusion- the spontaneous movement under the influence of concentration gradient (i.e., from regions of high concentration to regions of lower concentration), aimed at minimizing concentration differences.
- Convection-transport to the electrode by a gross physical movement; such fluid flow occurs with stirring or flow of the solution and with rotation or vibration of the electrode (i.e., forced convection) or due to density gradients (i.e., natural convection);

- Migration-movement of charged particles along an electric field (i.e., the charge is carried through the solution by ions according to their transference number).

3.1. 2. Electrode transfer reactions

Electrode reactions are heterogeneous and take place in the interfacial region between electrode and solution, the region where charge distribution differs from that of the bulk phases. The electrode process is affected by the structure of this region. The electrode can act as only a source (for reduction) or a sink (for oxidation) of electrons transferred to or from species in solution, as in ($O + ne^- \rightarrow R$) where O and R are the oxidized and reduced species, respectively. Alternatively, it can take part in the electrode reaction, as in dissolution of a metal M ($M \rightarrow M^{+n} + ne^-$).

In order for electron transfer to occur, there must be a correspondence between the energies of the electron orbitals where transfer takes place in the donor and acceptor.

Thus:

• for a reduction , there is a minimum energy that the transferable electrons from the electrode must have before transfer can occur, which corresponds to a sufficiently negative potential (in volts)

• for an oxidation , there is a maximum energy that the lowest unoccupied level in the electrode can have in order to receive electrons from species in solution, corresponding to a sufficiently positive potential (in volts).

3. 2. Electrochemical techniques

3. 2.1 Cyclic voltammetry (CV)

Cyclic voltammetry is the most widely used technique for acquiring qualitative information about electrochemical reaction. The effectiveness of CV results from its capability for rapidly observing redox behavior over a wide potential range. The resulting voltammogram is analogous to a conventional spectrum in that it conveys information as a function of energy scan.

CV consists of scanning linearly the potential of a stationary working electrode (in an unstirred solution), using a triangular potential wave form (Fig. 3.). Depending on the information sought single or multiple cycle can be used. During the potential sweep, the potentiostate measures the current resulting from the applied potential. The cyclic voltammogram is a complicated, time dependent function of a large number of physical and chemical parameter.

CV offers a rapid location of redox potentials of the electroactive species (ORR) and a convenient evaluation of the effect of media on redox process.

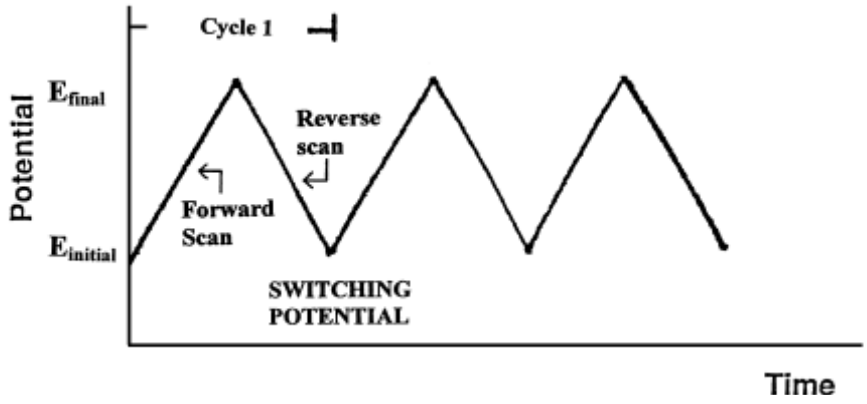

Fig. 3 potential-time exitation signal in cyclic voltammetric experiment

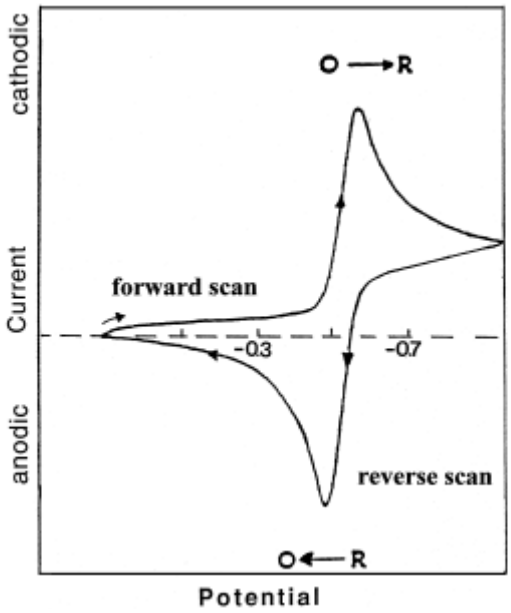

Fig. 4 Cyclic voltammogram for a reversible $O + ne^- \rightleftharpoons R$ redox process

A cyclic voltammogram (Fig. 4.) can quickly show the presence of all the species that undergo redox reaction at the electrode within the limit set by the solvent, electrolyte and the electrode [27].

3. 2. 2 Rotating disk voltammetry (RDV)

Rotating disk electrode technique has become one of the most extensively used techniques for investigating the mechanism and kinetics parameters of a variety of electrochemical reaction. Its major advantage over other methods lies in its ability to separate, through suitable mathematical apparatus, the diffusion component of the current from its kinetic part so that the analysis of each separate component can be made, leading to the determination of some overall kinetic parameters. In this manner the number of electron exchanged per molecule of reactant, the overall order of the reaction and the overall reaction rate constant have been determined for the number of process. This technique has also been extensively used in the determination of the mechanism of oxygen reduction and together with the rotating ring – disk technique has led to some important conclusion about the specific steps in oxygen reduction.

Rotating disk voltammetry provides much more quantitative information because electrolysis occurs under forced convection. In this technique, the electrode is rotated at an angular velocity of ω and the mass transfer limited current (i_L) depends only on the angular rotation velocity according to the following equation :

$$i_L = 0.62\ n\ F\ D^{2/3}\ C\ \nu^{-1/6}\ \omega^{1/2} \qquad (30)$$

Here n is the number of electron transferred, F is Faraday constant, A is electrode area, ν is kinematics viscosity , and D is the diffusion constant .

A linear plot of i_L Vs $\omega^{1/2}$ (a Levich plot) implies that the electrocatalytic reaction is faster than the rate of substrate delivered to the electrode, so that the current is determined only by how fast the substrate is transported to the surface. Since products of the electrode process are quickly transported out of the vicinity of the electrode disk, use of the rotating disk electrode complements the more complex rotating ring disk electrode

(RRDE). Here, redox active products can be detected at the ring electrode, which is held at a separately controlled potential.

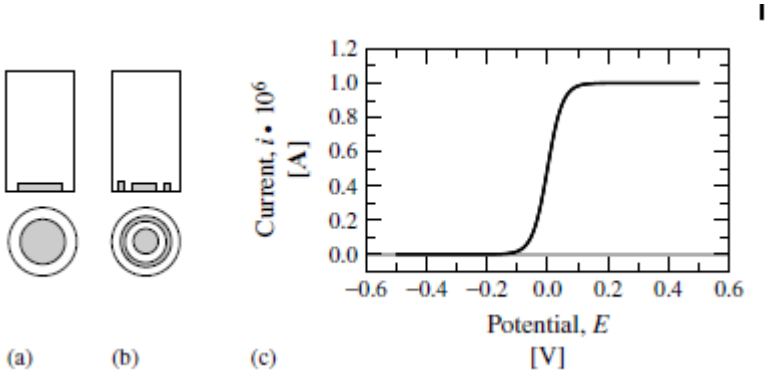

Fig. 5 Construction [section and bottom view, (a) RDE; (b) RRDE] of rotating disk electrodes; and (c) typical RDE response.

The kinetic contribution to the current on polymer modified electrode is given by:

$$i_k = nFAKC\Gamma \quad (31)$$

where K is the rate constant and Γ is the surface coverage of the electroactive electrode. The surface coverage can be evaluated from the equation $\Gamma = Q/nFA$

Combining Eq. 30 & 31 leads to the Koutecky-Levich expression, which describes the overall RDE plateau current for the electrocatalytic reaction:

$$1/i = 1/i_L + 1/i_K \quad (32)$$

According to this expression , a plot of $1/i_L$ Vs $\omega^{-1/2}$ should yield a straight line whose slope is related to the number of electron transferred (n) and whose intercept corresponds to the reciprocal kinetic current ($1/i_K$) [27-28].

3.2.2.1 General behavior of the modified electrode at a rotating disk

In general, a complex structure is designed toward a particular end, perhaps to facilitate an electrode process, or to inhibit a reaction, or to produce selectivity toward a particular process. The following scheme (Fig. 6.) shows processes that can occur at a modified electrode.

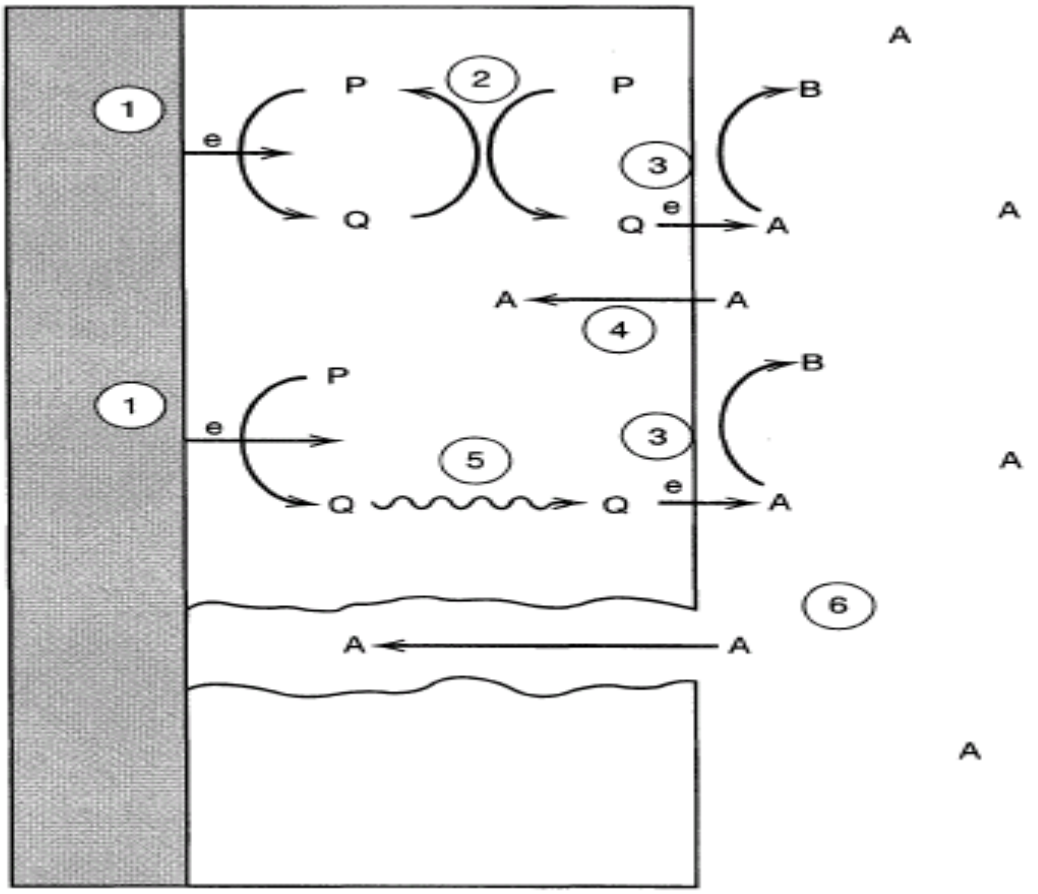

Fig. 6 Schematic diagram of processes that can occur at a modified electrode.

P represents a reducible substance in a film on the electrode surface and A, a species in solution. Processes shown are:

(1) heterogeneous electron transfer to P to produce the reduced form, Q;

(2) electron transfer from Q to another P in the film (electron diffusion or electron hopping in the film);

(3) electron transfer from Q to A at the film/solution interface;

(4) penetration of A into the film (where it can also react with Q or at the substrate-film interface);

(5) movement (mass transfer) of Q within the film;

(6) movement of A through a pinhole or channel in the film to the substrate, where it can reduced

A Koutecky-Levich plot **(**1/ i Vs $\omega^{-1/2}$) allows one to separate the effects of rate limitation within the film from those of convective diffusion outside. This plot is a convenient means for extrapolating behavior to infinite ω, and it yields $1/i_K$ as intercept**.**

The power of this approach in dealing with modified electrode lies in its generality. The treatment does not require any assumption about the identity of the rate limiting processes within the film. Several different types of activity can affect the rate at which A is converted to B. Species A must arrive at the film-solution boundary by convective diffusion; it might enter the structure by rate limited partitioning; it might require diffusion to the electrode surface or to a redox site within the film; there might be a rate limitation in the transfer of electrons at the electrode surface or at the redox site; and there might be a need for electrons to distribute themselves among redox sites throughout the structure. Any of these processes might be rate controlling for the overall conversion. In real systems, one also has to recognize the possibility of pores or pinholes in the film through which A can diffuse to the electrode [26].

A more general analysis involves separating contribution of electron transfer from other limiting activity inside the film.Therfore the Koutecky-Levich equation ($1/ i = 1/ i_L + 1/i_K$) can be re written as :

$$1/ i = 1/ i_l^{diff} + 1/i_l + 1/i^o \exp (|\eta| / b) \quad (33)$$

The equation assumes the electron transfer step is the rate determining and occur at large overvoltage

Where i_l^{diff} limiting current density for the diffusion in the bulk electrolyte

i_l limiting current density resulting from a mixed control inside film other than electron transfer at the electrode(Since this current is independent of ω and E, it is not possible to separate their contribution)

η the overvoltage (E – E eq)

The intercept at the origin ($\omega \rightarrow \infty$) of Koutecky-Levich plot **(**1/ i vs $\omega^{-1/2}$) gives the inverse of the kinetic current, as a function of the overvoltage, i.e.:

$$1/i_K = 1/i_l + 1/i^o \exp(|\eta| / b) \quad (34)$$

Eq. (34) thus shows that for high overvoltage ($|\eta| \rightarrow \infty$) the quantity $1/ i_K$ tends towards $1/ i_l$, so that one can obtain the limiting current density i_l by extrapolating eq. (34) at high η.This allowed as to transform eq (34) as follows:

$$\eta = E - E_{eq} = b \left[\ln | i_K / i_l - i_K | + \ln i_l / i^o \right] \quad (35)$$

Plotting $1/i_k$ as a function of electrode potential E, allowed as determining limiting current (i.e. resulting from a mixed control inside the polymer). Knowing i_l it is possible to plot $\ln [i_k / (i_k - i_l)]$ vs the overpotential η gives a straight line with a slope 1/ b and an intercept at the origin $[-\ln (i_l / i^o)]$.From this results Tafel slope (b) and i^o can be calculated [29].

3. 3. Electrochemical process [27, 30 & 31]

The success of an electrolysis process depends on the choice of a suitable electrochemical cell and optimal operation conditions because there is a widespread variety of electrolyte composition, cell constructions, electrode materials, and electrochemical reaction parameters.

3.3.1 Electrochemical cell

Three-electrode cells (e.g., Fig.7.) are commonly used in controlled – potential experiments. Three electrodes are usually employed: a working (indicator), reference and counter (Auxiliary) electrodes.

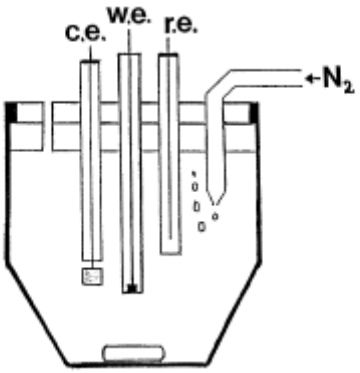

Fig. 7. Schematic diagram of a cell for voltammetric measurement: w.e.,working electrode; r.e.,reference electrode; c.e.,counter electrode. The electrodes are inserted through holes in the cell cover.

Fig. 8. A complete cell stand

A. Working electrodes

It is the electrode at which the reaction of interest occurs. The performance of the voltammetric procedure is strongly influenced by the working electrode material.

A wide range of solid materials are used as electrodes. The most common 'inert' solid electrodes are lead, vitreous carbon (glassy carbon), gold and platinum.

Glassy carbon has been very popular because of its excellent mechanical and electrical properties, wide potential window, chemical inertness (solvent resistance) and relatively reproducible performance.

Electrode pretreatment are always needed in order to get reproducible data on solid electrodes. They are mostly focused on the removal of surface impurities (oxides). Electrodes can be polished with alumina of fixed grain size down to 0.05μm.

B.Counter electrode

The purpose of the counter electrode is to supply the current required by the working electrode without in any way limiting the measurement response of the cell. It is the current carrying electrode and must be inert and larger in dimension. Platinum wire or foil is the most common counter electrode.

C. Reference electrode

The role of the reference electrode is to provide a fixed potential which does not vary during the experiment. Some typical reference electrodes are presented in Table 1.

Table 1. Potential of some typical reference electrodes in aqueous solution at 298k

Common name	electrode	Potential Vs NHE
SCE(saturated)	Hg/Hg_2Cl_2, sat KCl	+0.241
Calomel	Hg/Hg_2Cl_2,1moldm^{-3} KCl	+0.28
Mercurous sulphate	Hg/Hg_2SO_4, sat K_2SO_4	+0.64
	Hg/Hg_2SO_4 0.5M H_2SO_4	+0.68
Mercuric oxide	Hg/HgO,1moldm^{-3} NaOH	+0.098
Silver chloride	Ag/AgCl, sat KCl	+0.197

3.3.2. The electrolyte solution

The electrolyte solution is the medium between the electrodes in the cell, and it will consist of solvent and a high concentration of an ionized salt (supporting electrolyte) as well as the electroactive species.

The supporting electrolyte is present:

- To increase the conductivity of the solution and hence to reduce the resistance between the working and the counter electrode.
- To effectively eliminate migration as a mode of mass transport for electroactive species.

3.3.3. Oxygen removal

The most common method has been purging with an inert gas (usually purified nitrogen) for 4-8 minutes prior to recording of the voltammogram.

4. OBJECTIVE OF THE STUDY

The objectives of the study were to examine the electrochemical behavior and the electrocatalytic activity of 4-amino-3-hydroxynaphtalene sulfonic acid (AHNSA), 2-aminobenzoic acid (ABA) and 8-aminonaphtalene-2-sulfonic acid (ANSA) modified glassy carbon electrodes using cyclic voltammetry and rotating disk Voltammetry. Furthermore, kinetic parameters of oxygen reduction reaction on 4-amino-3-hydroxynaphtalene sulfonic acid (AHNSA), 2-aminobenzoic acid (ABA) and 8-aminonaphtalene-2-sulfonic acid (ANSA) modified glassy carbon electrodes were compared based on both the exchange current density and Tafel slope.

5. EXPERMENTAL

5.1 Chemical and solution

All chemical and reagents used were analytical grade, Al_2O_3 (Riedel-de Haen) was used for polishing the electrode surface. Distilled water and HNO_3 were used to prepare the solutions. Supporting electrolyte used for electrochemical experiment was 0.5M H_2SO_4.The aqueous solutions were prepared by distilled water and before each experiment the solution were deoxygenated for 10 minutes by purging with argon gas with an exception of O_2 reduction reaction. Pure oxygen gas (product of Chora gas and chemical products) from a cylinder was purged into 0.5M H_2SO_4 for about 20 minutes inorder to saturate a 0.5M H_2SO_4 supporting electrolyte for all oxygen reduction reaction. The concentration of oxygen in an oxygen saturated 0.5M H_2SO_4 solution is 1.03×10^{-3} M [32].

5. 2. Apparatus

Electrochemical measurement were performed using voltammetric analyzer (BAS-CV-5OW) using a conventional three electrode system. Glassy carbon with 3mm in diameter was used as working electrode, platinum wire as counter electrode. All the cell potentials were measured with respect to an Ag/AgCl [KCl (3M)] reference electrode. Hydrodynamic voltammetric studies on oxygen reduction reaction were performed on episilon voltammetric analyzer having an analytical rotator. An electronic digital balance was used to measure the weights of solid chemicals during solution preparation.

5.3. Preparation of the modified electrode

Prior to use, the working electrodes were mechanically polished with alumina powder (Al_2O_3, 0.05μm) upto a mirror finish. Then the electrodes were cycled in 0.5M H_2SO_4 in

a potential range from -0.8V to 0.8V at a sweep rate 100mV/s until a stable voltammogram was obtained.

The electrochemical deposition of 4-amino-3-hydroxynaphtalene sulfonic acid (AHNSA), 2-aminobenzoic aid (ABA) and 8-aminonaphtalene-2-sulfonic acid (ANSA) films were carried out by cyclic voltammetry between -0.8V and 2.0V at 10mV/s for 20 cycles.

The electropolymerization was conducted in a three electrode cell with glassy carbon electrode as the working electrode Ag/AgCl as the reference electrode and platinum wire as the counter electrode.

The electrolyte consisted of 2mM (4-amino-3-hydroxynaphtalene sulfonic acid (AHNSA) , 2-aminobenzoic acid (ABA) and 8-aminonaphtalene-2-sulfonic acid (ANSA) of each monomer in aqueous solution of 0.1M HNO_3, The resulting films were washed with distilled water before proceeding electrochemical measurement. Finally, the modified GC electrodes were activated by cyclic voltammetry from -0.8V to 0.8V in 0.5M H_2SO_4.

6. RESULTS AND DISCUSSION

6.1 Electrocatalytic reduction of oxygen on 4-amino-3- hydroxyl Naphtalene sulfonic Acid (AHNSA)

6.1.1 Cyclic voltammetry

The reduction of oxygen saturated in 0.5M H_2SO_4 supporting electrolyte was investigated at GC/AHNSA. The current vs potential curve (Fig. 9.) were recorded during a slow voltammetric sweep (sweep rate 10mV/s)

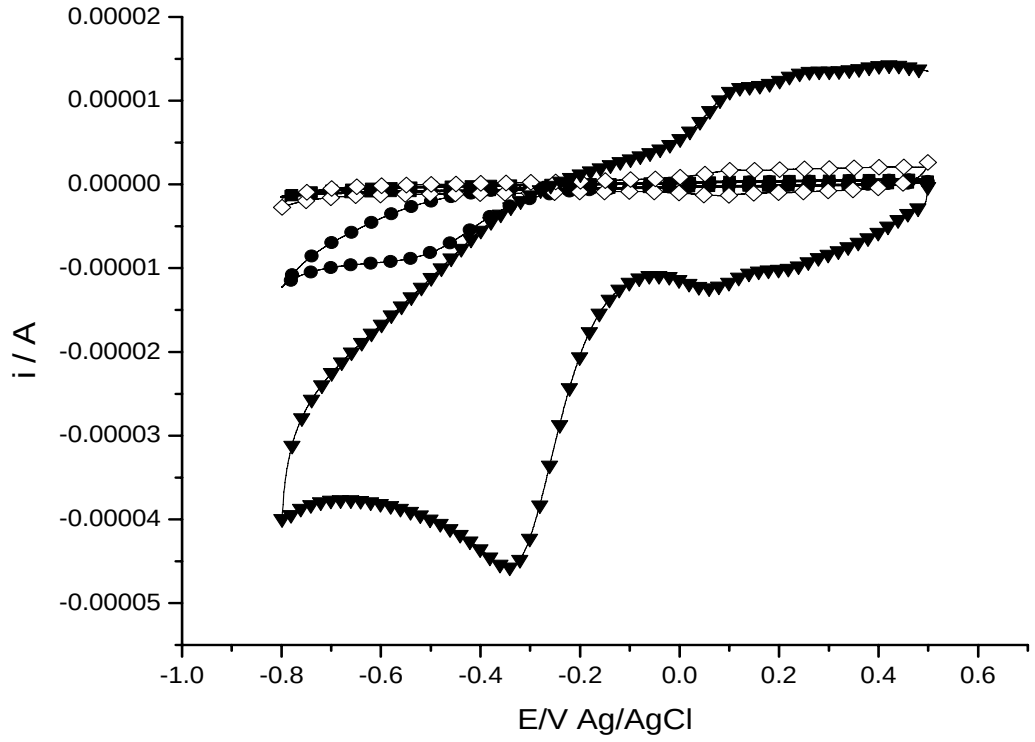

Fig. 9 CVs of : bare GC electrode in argon (■), bare GC electrode in O_2 saturated (●), Argon saturated GC/AHNSA (◊) and O_2 saturated GC/AHNSA (▼) (O_2 saturated 0.5M H_2SO_4, 10mV/s)

In the presence of O_2 a new peak was developed at -340 mV. This cathodic peak corresponds to the electrochemical reduction of oxygen at the GC/AHNSA electrode (Fig. 9 curve ▼).The electrochemical reduction of oxygen at a bare GC electrode shows a broad ill defined cathodic peak (curve ●) and the cathodic peak potential is located at about -541mV. Based on the above results, it was concluded that GC/AHNSA electrode reduced the overpotential required for O_2 reduction about 200mV. Furthermore, the peak current of curve (●) is much less than that in Fig. 9 curve (▼).

All the above results indicated that the GC/AHNSA electrode has excellent electrocatalytic activity for the electrochemical reduction of O_2.

6.1. 2 Oxygen reduction reaction at AHNSA modified rotating disk glassy carbon Electrode

The reduction of oxygen saturated in 0.5M H_2SO_4 supporting electrolyte was investigated at GC /AHNSA rotating disk electrode for several rotation speeds ω (from 100 to 3200 rpm).The current vs potential curve (Fig. 10.) were recorded during a slow voltammetric sweep (sweep rate $10mVs^{-1}$**).**

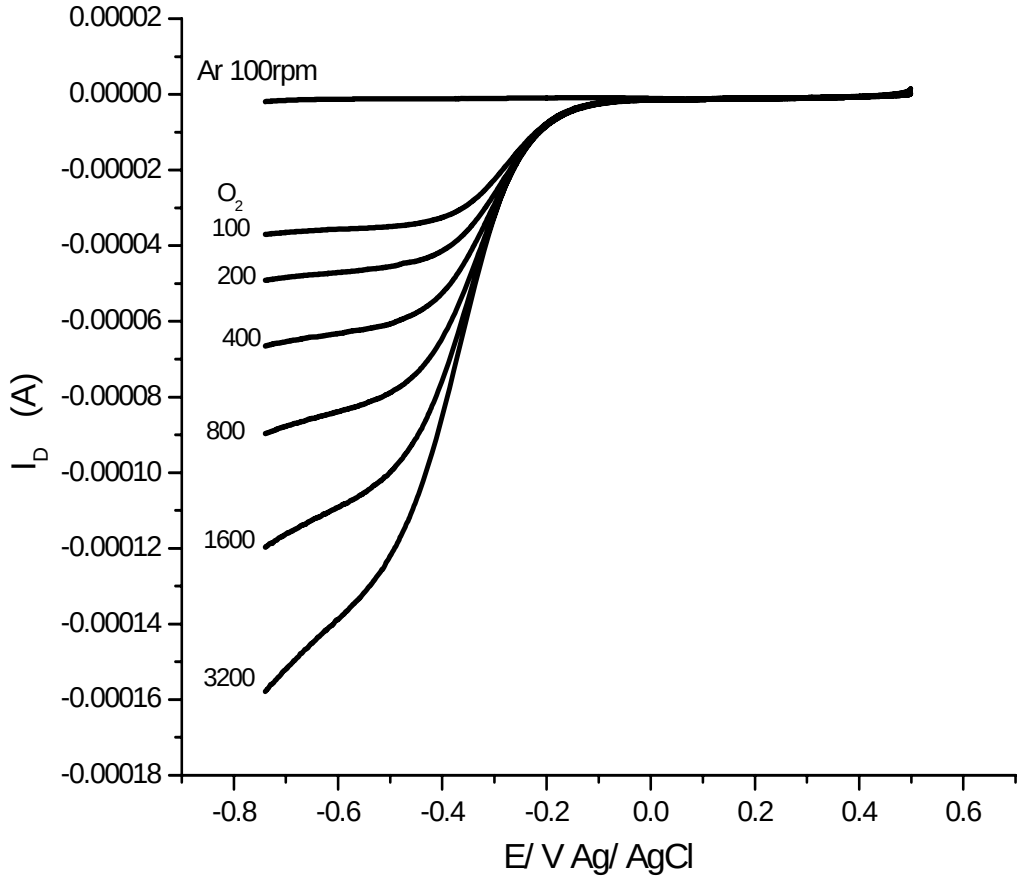

Fig. 10 Rotating disk voltamograms for reduction of oxygen (1.03mM) at AHNSA/GC disk electrode for six different rotation speeds (O_2 saturated 0.5M H_2SO_4, 10mV/s).

In Fig.10 the onset of oxygen reduction was observed at about -0.2V vs Ag/AgCl and plateau region was observed. The limiting current was observed and increased with the rotation speed. A Levich plot (i_d vs $\omega^{1/2}$) for oxygen reduction reaction at AHNSA modified glassy carbon electrode in an O_2 saturated 0.5M H_2SO_4 solution is shown in Fig.11

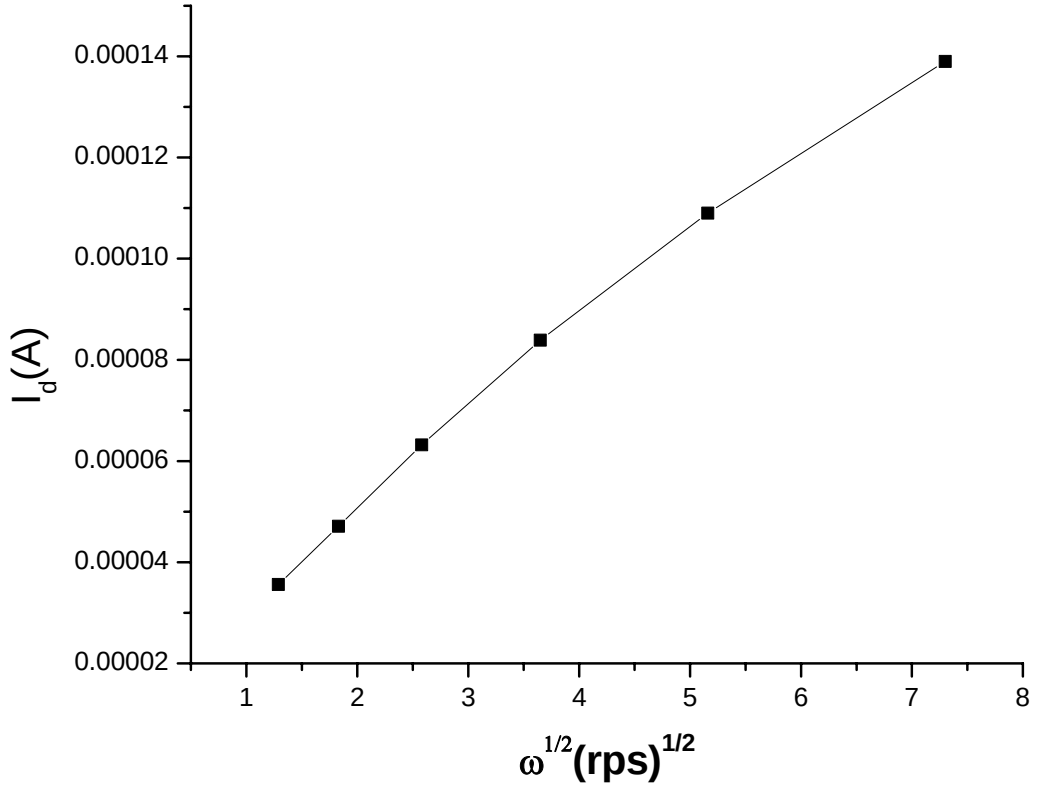

Fig. 11 Levich plots for the reduction of oxygen at AHNSA modified glassy carbon electrode (O_2 saturated 0.5M H_2SO_4,10mV/s)

In Fig. 11 the Levich plot derived from the limiting current at a potential of -0.6 V is non linear for a reaction in which a current limiting chemical step precedes the electron transfer .The Levich plots (Fig. 12.) is very close to the theoretical calculated line for a four electrons process (n = 4) which indicates the accomplishment of the reduction of O_2 to H_2O.

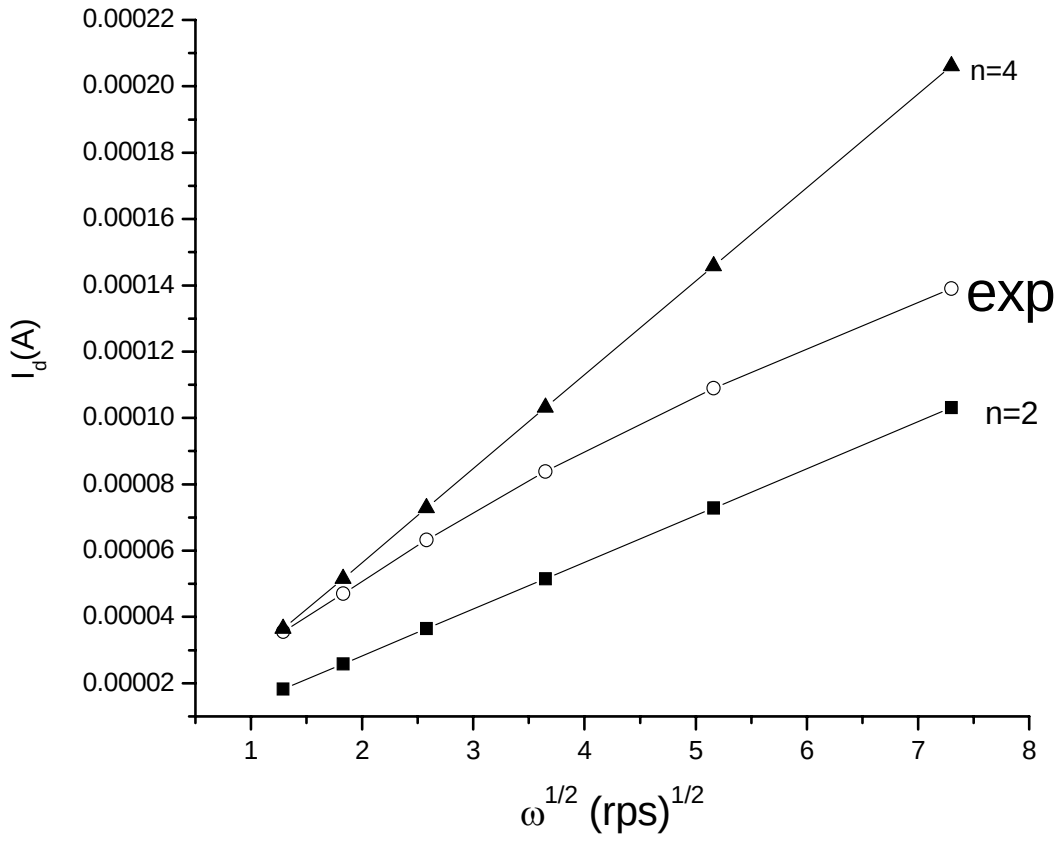

Fig. 12 Levich plots for the reduction of oxygen at AHNSA modified glassy carbon electrode (O_2 saturated 0.5M H_2SO_4,10mV/s) for theoretical (2es and 4es) and experimental result.

The values used for calculation of theoretical Levich plots were: D = 2.1×10^{-5} cm^2 / s for the diffusion coefficient of molecular oxygen,ν = 1.075 x 10^{-2} cm^2 / s for the kinematic viscosity of oxygen and Co = 1.03mM for the concentration of oxygen in 0.5M O_2 saturated H_2SO_4 [32], the Faraday constant, F = 96485 C/mol and area of the disk electrode, A= 0.0707cm^2 geometric surface area. The corresponding Koutecky-Levich (Fig. 13) plot also confirms the reduction of O_2 to H_2O. The experimental value of the slope is 0.0341 μA $(rps)^{-1/2}$ agrees reasonably well with the theoretical value (0.0354μA $(rps)^{-1/2}$) for four electron process.

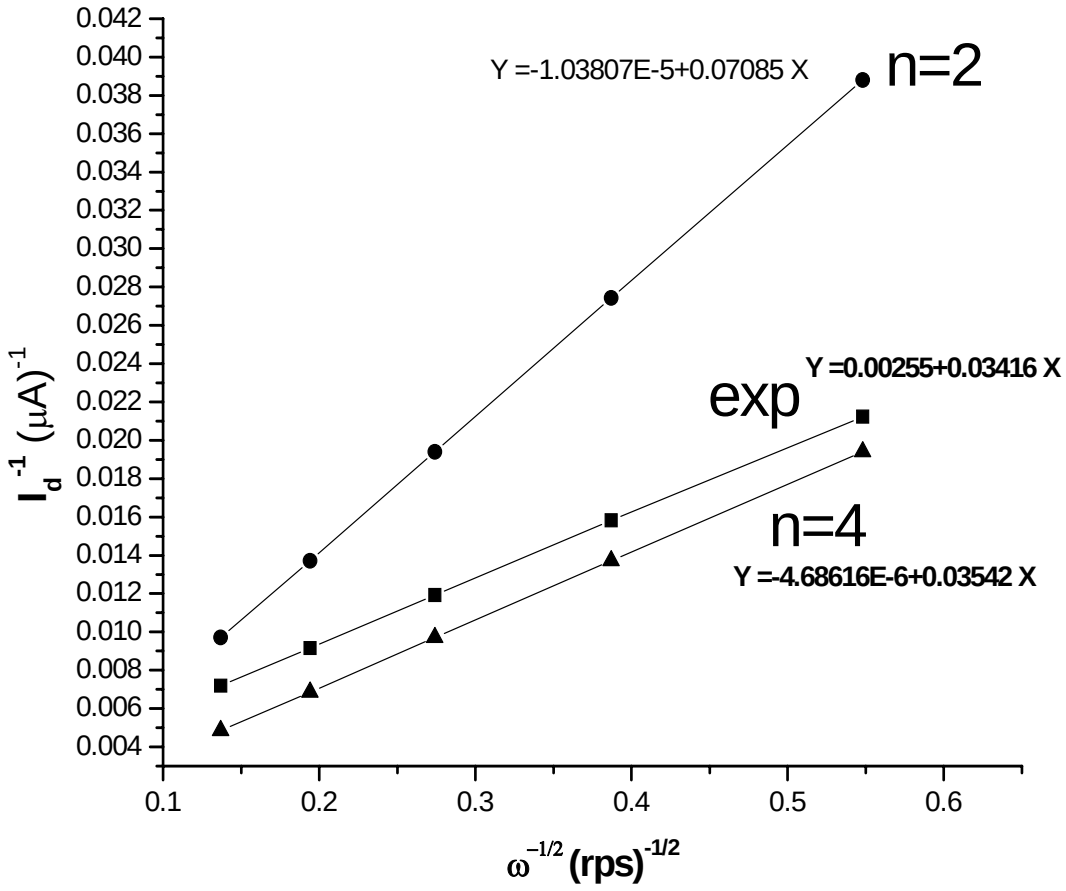

Fig. 13 Koutecky- Levich plots i^{-1} vs $\omega^{-1/2}$ for the reduction of oxygen on AHNSA/GC rotating disk electrode (O_2 saturated 0.5M H_2SO_4, 10mV/s) for theoretical (2es and 4es) and experimental result.

Plots of i^{-1} vs $\omega^{-1/2}$ at various potential (Fig. 14) yielded parallel straight lines. The slopes remain constant over the potential range (-0.45V - 0.7V) indicating a constant value of number of electrons involved in the reduction reaction. The result shows a first order kinetics with respect to the diffusion of the reactant.

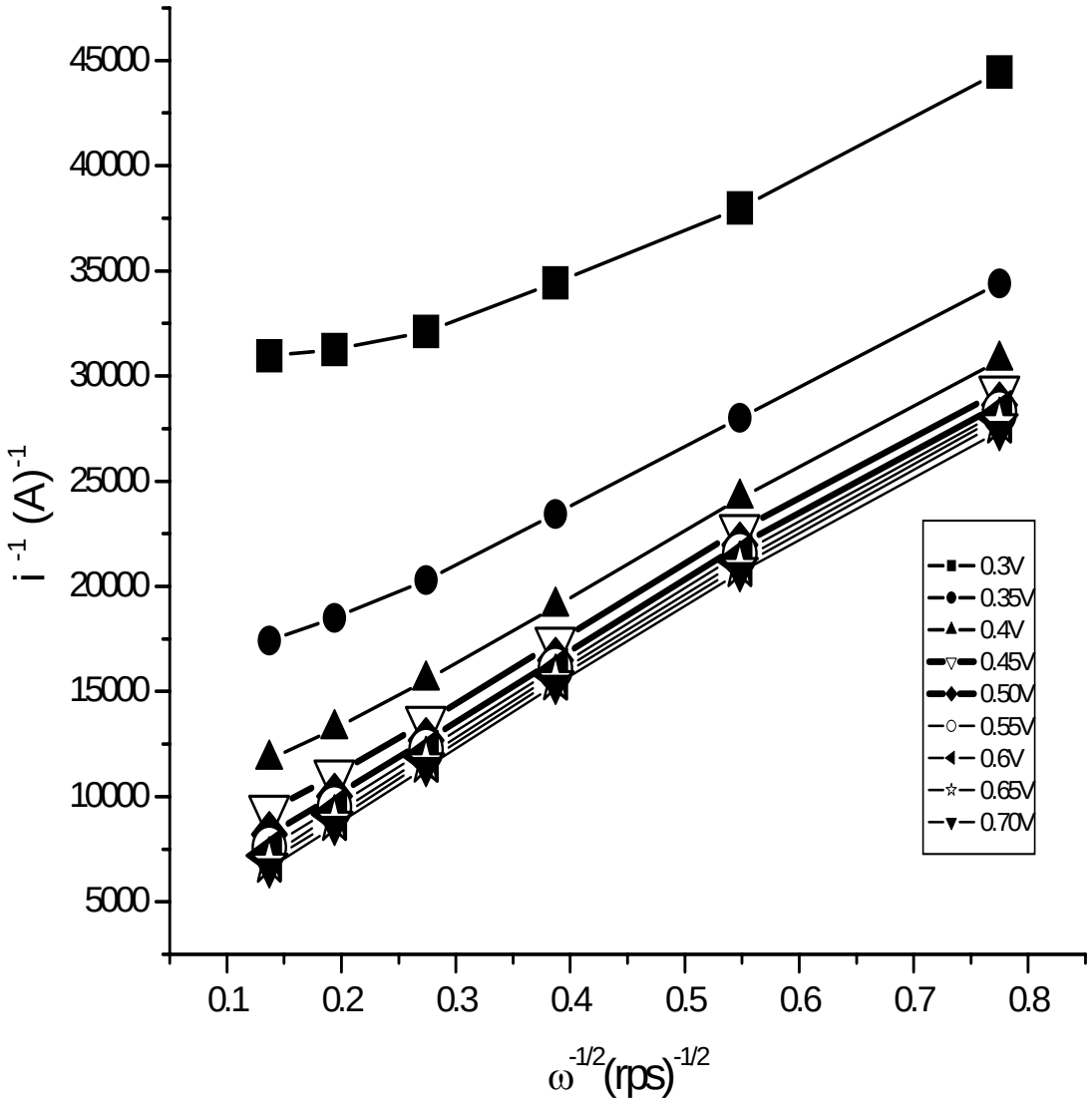

Fig. 14 Koutecky-Levich plots i^{-1} vs $\omega^{-1/2}$ for the reduction of oxygen on AHNSA/GC rotating disk electrode (O_2 saturated 0.5M H_2SO_4, 10mV/s) at a different potential.

As represented in Fig. 14 plots of i^{-1} vs $\omega^{-1/2}$ give good linearity. If the disk potential (E_D) shifts from less negative (-0.3V) to more negative (-0.7V) the intercept of the i^{-1} vs

$\omega^{-1/2}$ Curves becomes smaller. This indicates that the catalytic reaction moves from a kinetically controlled process to a mass transport controlled process. The kinetic contribution to the total current increases if the disk potential moves from less negative to more negative values. As the potential is become more negative it would be more favorable for the electron transfer process.

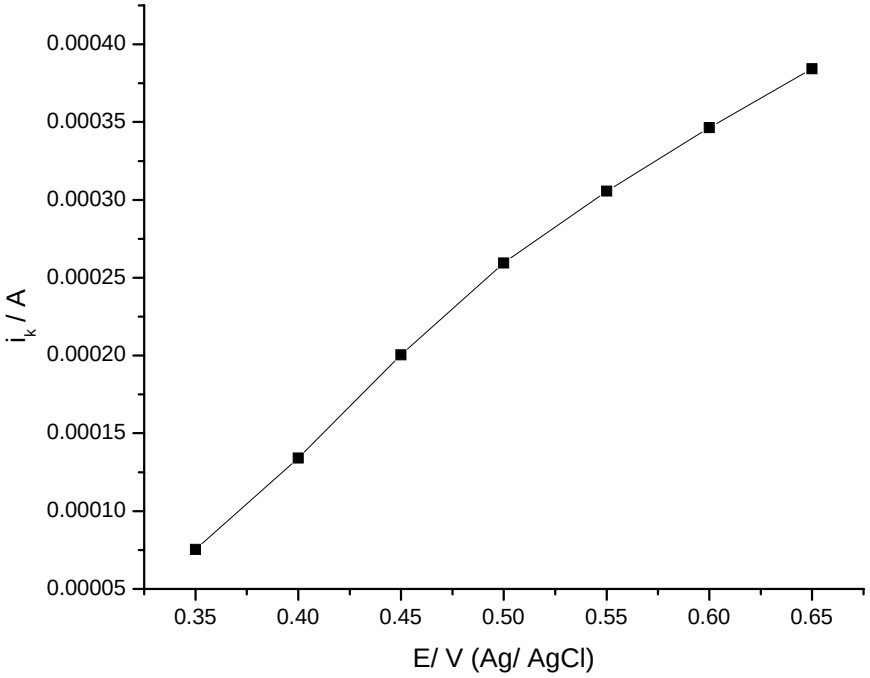

Fig. 15 Plot of i_k vs potential for the reduction of oxygen on AHNSA/GC rotating disk electrode (O_2 saturated 0.5M H_2SO_4, 10mV/s) at a different potential.

Plot of $1/ i_k$ vs the electrode potential (E) Fig. 16 allows to determine the limiting current density (per geometric surface area) resulting from a mixed control (i_l) obtained by extrapolating eq. (34) at high η. The value of $1/i_l$ obtained was 169.54 cm^2A^{-1} and i_l for AHNSA / GC modified electrode was found to be $5.89x10^{-3}Acm^{-2}$.

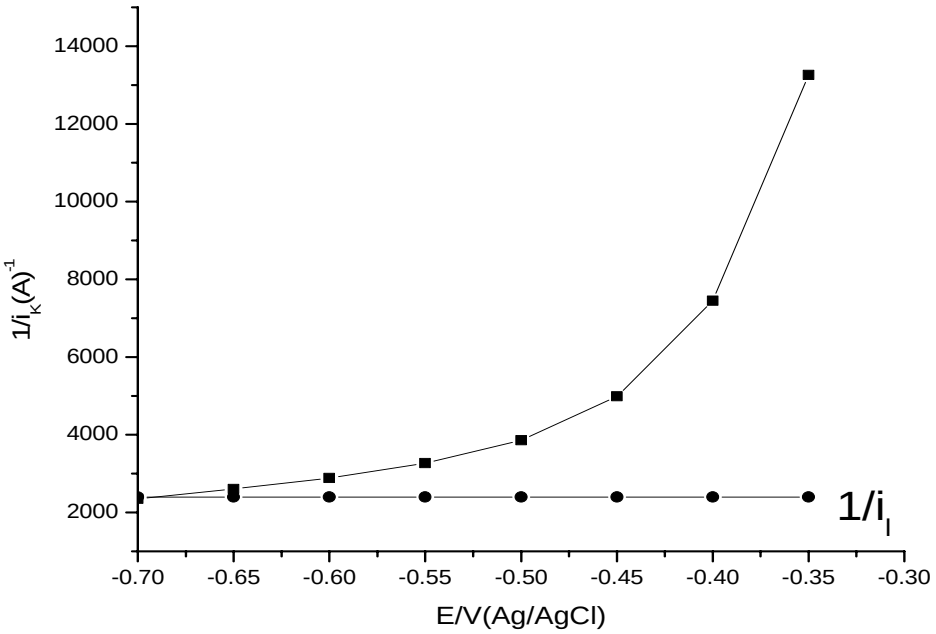

Fig. 16 Plot of $1/ i_k$ vs the electrode potential for the reduction of oxygen on AHNSA modified glassy carbon rotating disk electrode(O_2 saturated 0.5M H_2SO_4, 10mV/s).

Knowing i_l it is possible to plot ln [i_k / (i_k - i_l)] vs E (Fig. 17) gives a straight line with a slope 1/ b (12.623 dec / V) and an intercept at the origin - ln (i_l / i^o) (-5.8506). From these results a Tafel slope 79.21mV/ dec and an exchange current density of 1.7 x 10^{-6}A/cm^2 were calculated. The limiting current density resulting from a mixed control (i_l) is much higher (by a factor of 3.4 x10^3 times) that of the exchange current density i^o. This confirms that the electron transfer step is rate determining.

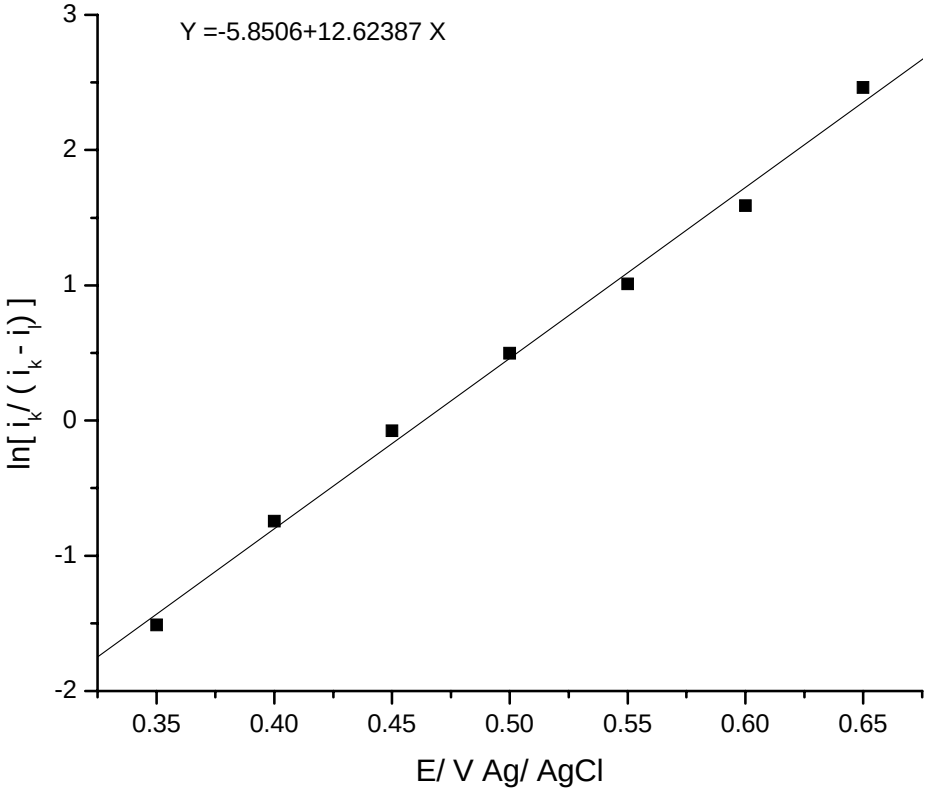

Fig. 17 Plot of $\ln[i_k/ (i_k - i_l)]$ vs the electrode potential (E) for the reduction of oxygen on AHNSA modified glassy carbon rotating disk electrode (O_2 saturated 0.5M H_2SO_4, 10mV/s).

6. 2. Electrocatalytic reduction of oxygen on 2-aminobenzoic acid (ABA)

6. 2.1.Cyclic voltammetry

The reduction of oxygen dissolved in 0.5M H_2SO_4 supporting electrolyte was investigated at GC/ABA. The current vs potential curve (Fig. 18) were recorded during a slow voltammetric sweep (sweep rate 10mV/s).

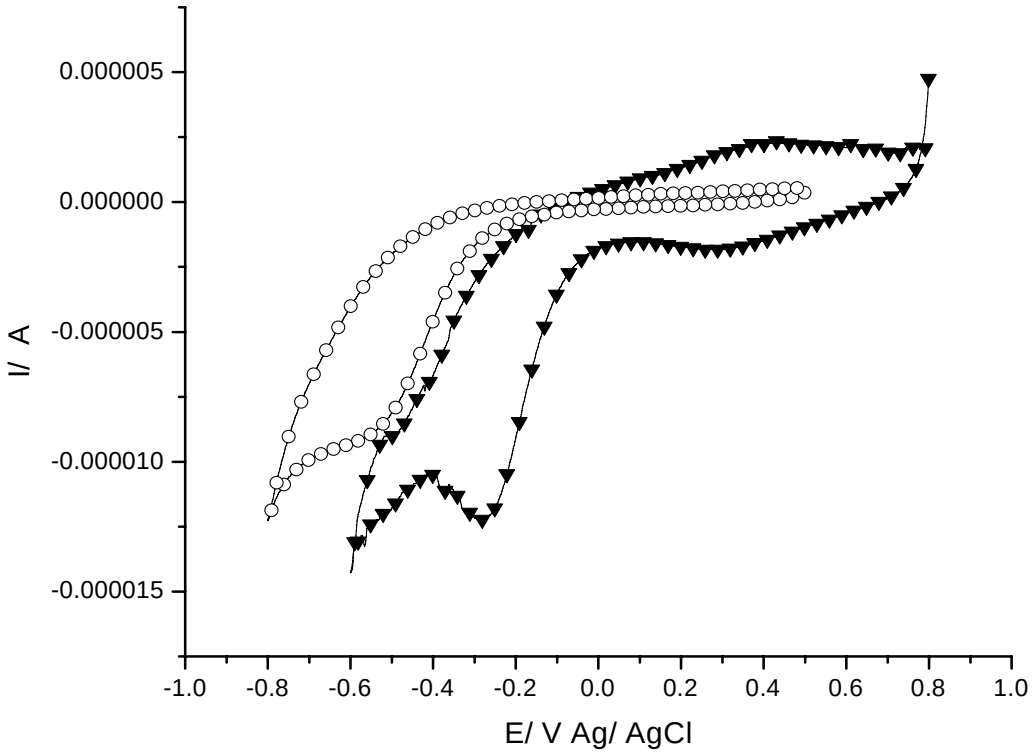

Fig. 18 CVs of: bare GC electrode in O_2 saturated (O), and O_2 saturated ABA/GC (▼) (O_2 saturated 0.5 M H_2SO_4,10 mV /s)

In the presence of O_2 a new peak was developed at -272 mV. This cathodic peak corresponds to the electrochemical reduction of oxygen at the ABA/GC electrode

(Fig. 18 curve ▼). The electrochemical reduction of oxygen at a bare GC electrode shows a broad ill defined cathodic peak (curve O) and the cathodic peak potential is located at about -541mV. Based on the above results, it was concluded that ABA/GC electrode reduced the overpotential required for O_2 reduction about 269 mV. Further more, the peak currents of curve (O) is less than that in curve (▼).

All the above results indicated that the ABA/GC electrode has electrocatalytic activity for the electrochemical reduction of O_2.

6. 2. 2. Oxygen reduction reaction at ABA modified rotating disk glassy carbon Electrode

The reduction of oxygen dissolved in 0.5M H_2SO_4 supporting electrolyte was investigated at ABA/GC rotating disk electrode for several rotation speeds ω (from 100 to 3200 rpm).The current vs potential curve (Fig. 19) were recorded during a slow voltammetric sweep (sweep rate $10mVs^{-1}$)**.**

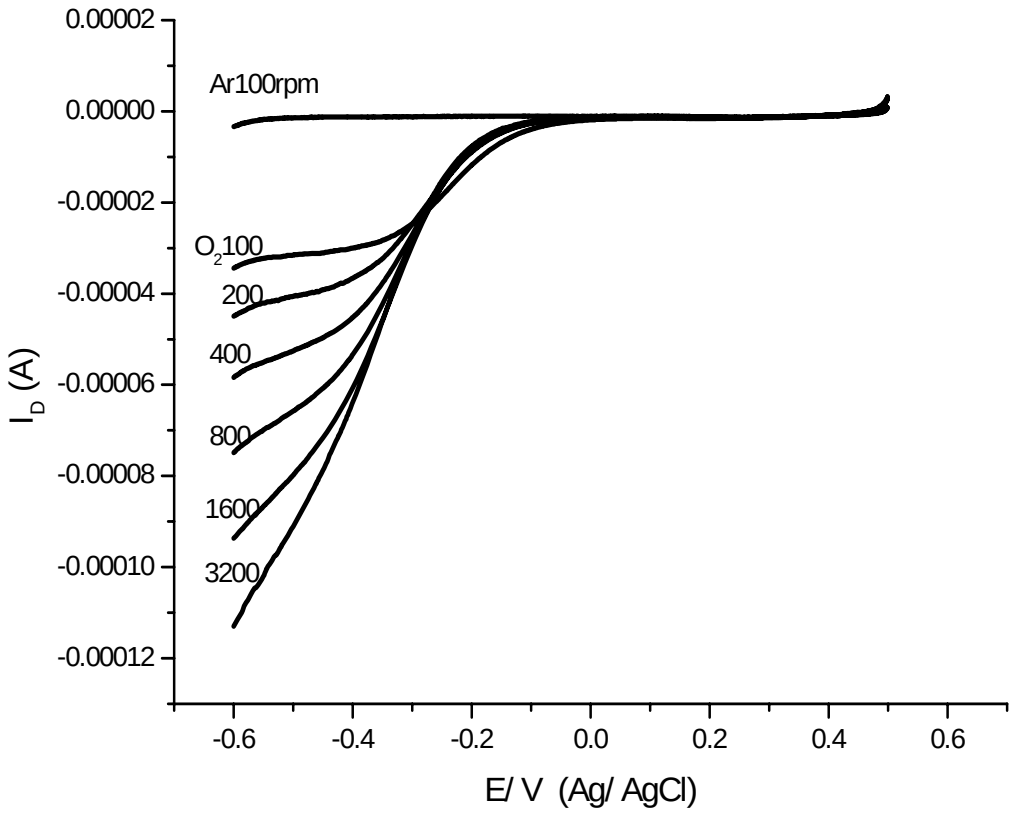

Fig. 19 Rotating disk voltamograms for reduction of oxygen (1.03mM) at ABA /GC disk electrode for six different rotation speeds (O_2 saturated 0.5M H_2SO_4, 10mV/s)

In Fig. 19 the onset of oxygen reduction was observed at about -0.1 V Vs Ag/AgCl and plateau region was observed. The limiting current was observed and increased with the rotation speed. A Levich plot (i_l vs $\omega^{1/2}$) for oxygen reduction reaction at ABA modified glassy carbon electrode in an O_2 saturated 0.5M H_2SO_4 solution is shown in Fig 20.

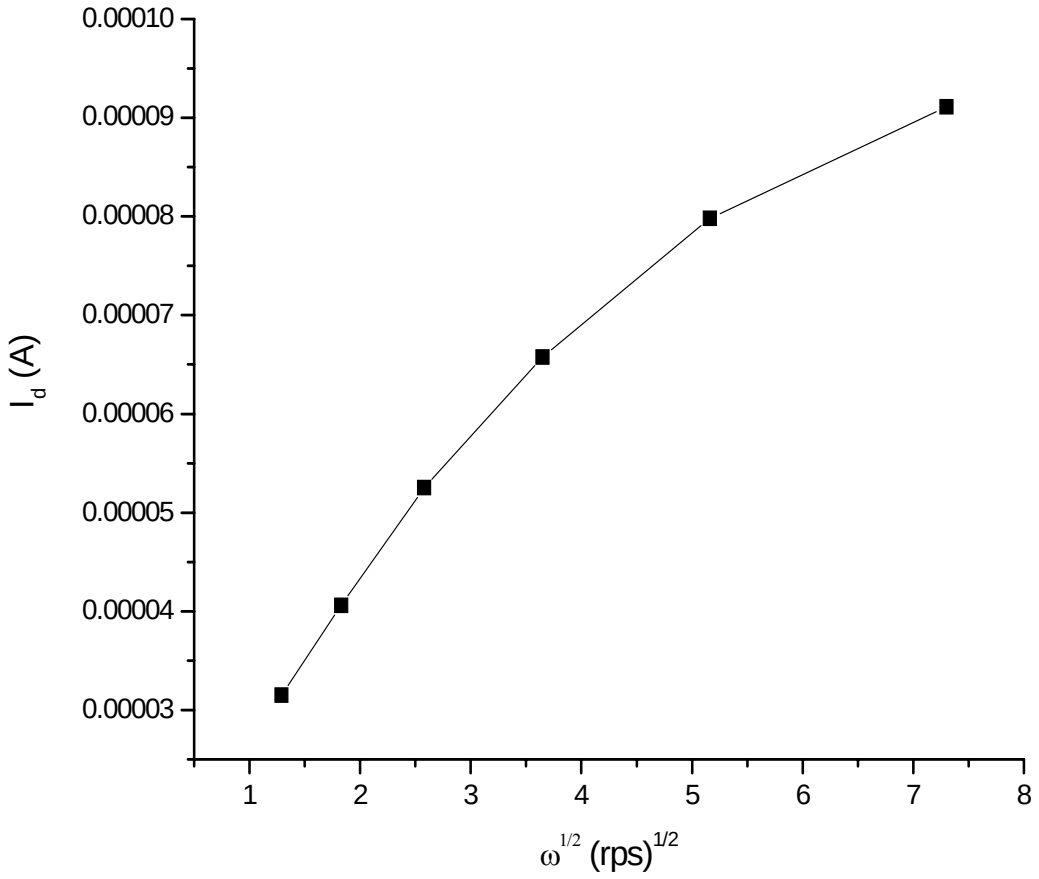

Fig. 20 Levich plot for the reduction of oxygen at ABA modified glassy carbon electrode (O_2 saturated 0.5M H_2SO_4,10mV/s)

In Fig. 20 the Levich plot derived from the limiting current at a potential of – 0.45 V is non linear for a reaction in which a current limiting chemical step precedes the electron transfer. The Koutecky-Levich plot (Fig. 21) is very close to the theoretical calculated line for a four electron process (n=4) which indicates the accomplishment of the reduction of O_2 to H_2O. The experimental value of the slope is 0.03122 μA (rps) $^{-1/2}$ agrees reasonably well with the theoretical value (0.0354 μA (rps) $^{-1/2}$) for four electrons process.

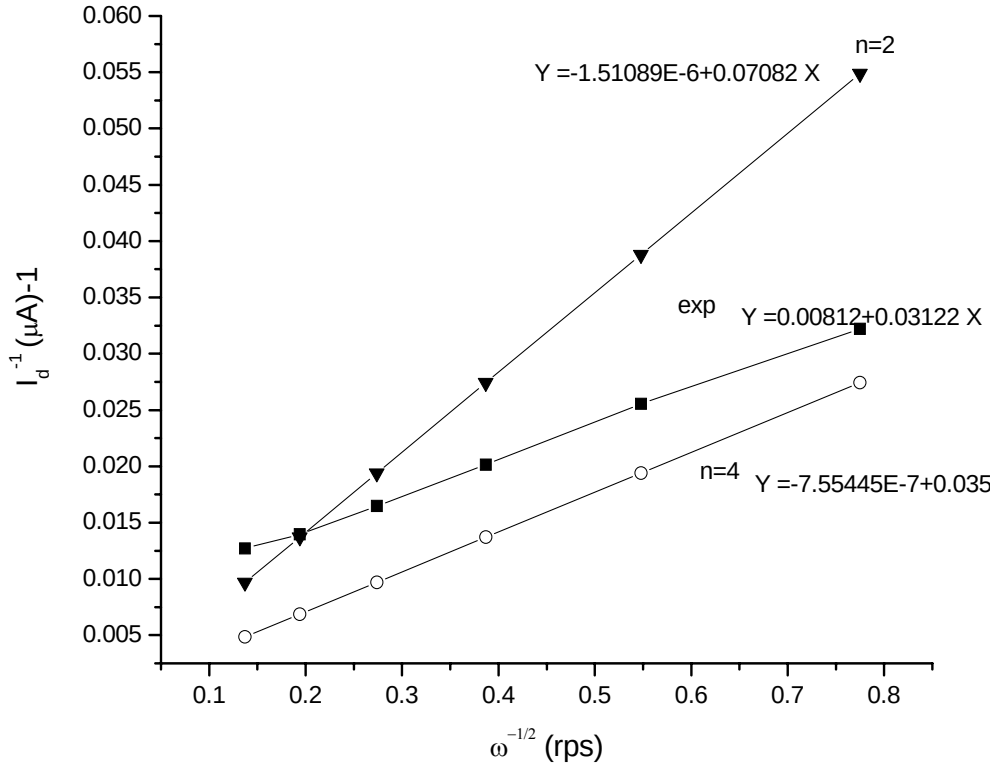

Fig. 21 Koutecky-Levich plots i^{-1} vs $\omega^{-1/2}$ for the reduction of oxygen on ABA /GC rotating disk electrode (O_2 saturated 0.5M H_2SO_4, 10mV/s) for theoretical (2es and 4es) and experimental result.

As represented in Fig. 22 plots of i^{-1} vs $\omega^{-1/2}$ give good linearity. If the disk potential (ED) shifts from less negative (-0.37 V) to more negative (-0.5V) the intercept of the i^{-1} vs $\omega^{-1/2}$ Curves becomes smaller. This indicates that the catalytic reaction moves from a kinetically controlled process to a mass transport controlled process.

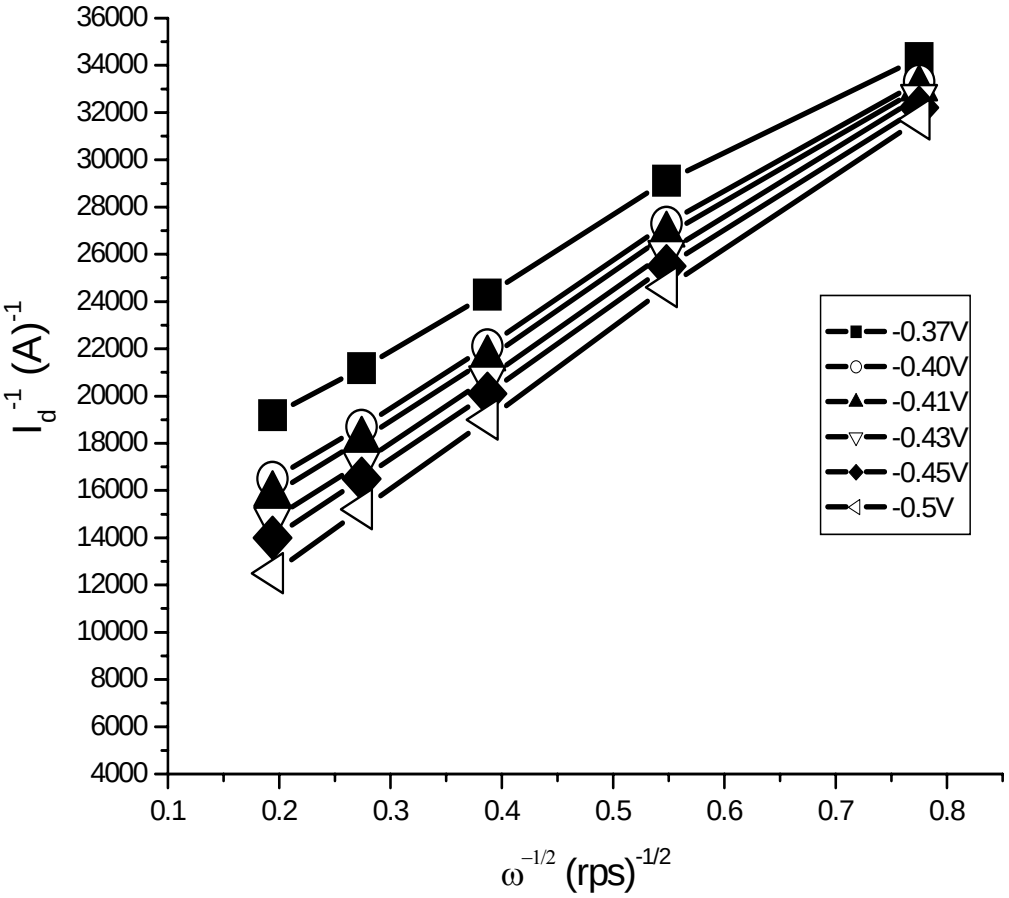

Fig. 22 Koutecky-Levich plots i^{-1} vs $\omega^{-1/2}$ for the reduction of oxygen on ABA /GC rotating disk electrode (O_2 saturated 0.5M H_2SO_4, 10mV/s) at a different potential.

Plots of i^{-1} vs $\omega^{-1/2}$ at various potential (Fig. 22.) yielded parallel straight lines. The slopes remain constant over the potential range (-0.37V - 0.5V) indicating a constant value of number of electrons involved in the reduction reaction. The result shows a first order kinetics with respect to the diffusion of the reactant.

The kinetic contribution to the total current increases if the potential moves from less negative to more negative values (Fig. 23). As the potential become more negative it would be more favorable for the electron transfer process.

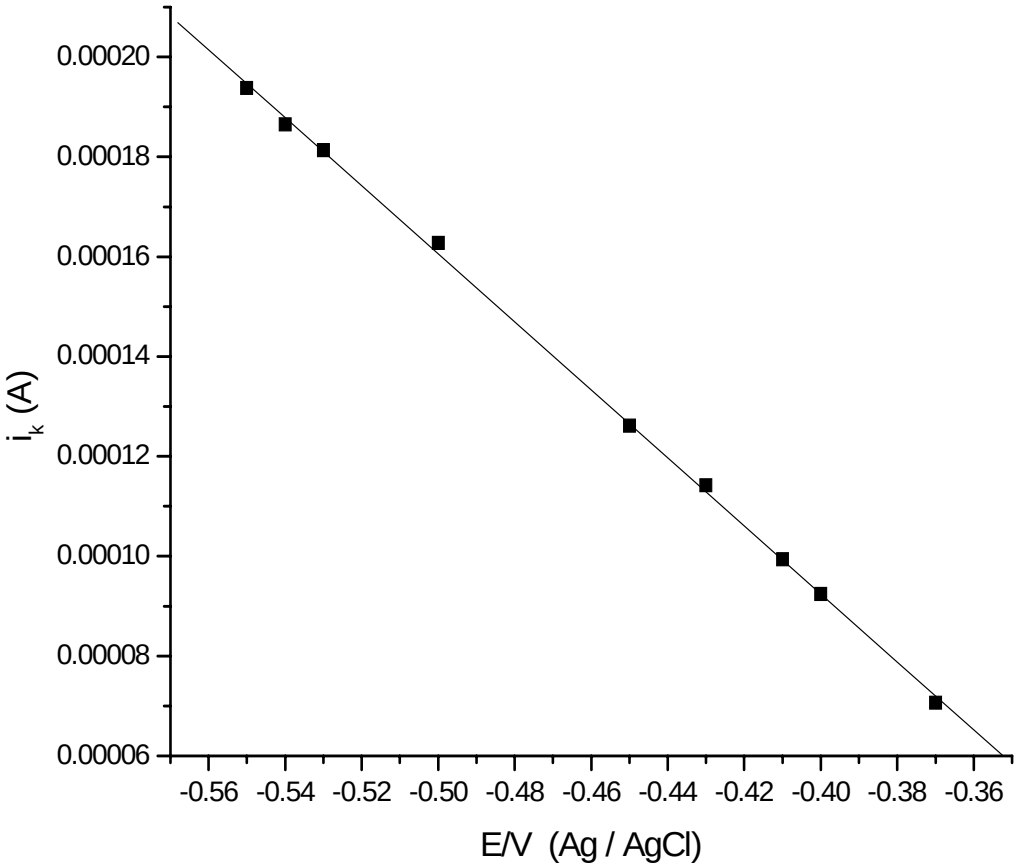

Fig. 23 Plot of i_k vs potential for the reduction of oxygen on ABA/GC rotating disk electrode (O_2 saturated 0.5M H_2SO_4, 10mV/s) at a different potential.

Plot of $1/ i_k$ vs the electrode potential (E) Fig. 24 allows to determine the limiting current density resulting from a mixed control (i_l) obtained by extrapolating eq. (34) at high η. The value of $1/i_l$ obtained was 364.43 $cm^2 A^{-1}$ and i_l for ABA/GC modified electrode was found to be 2.74 x 10^{-3} A/cm^2.

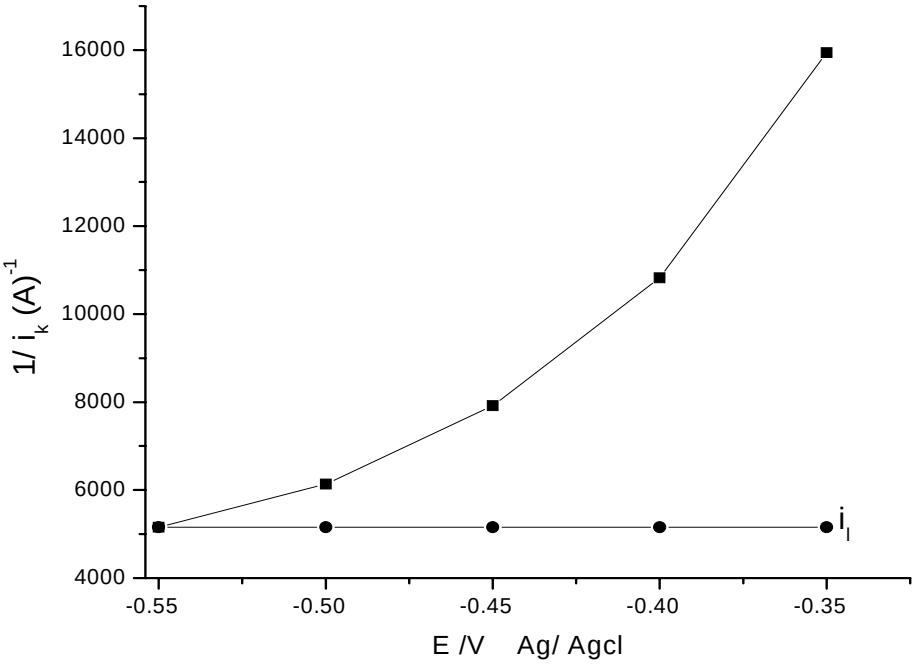

Fig. 24 Plot of $1/ i_k$ vs the electrode potential for the reduction of oxygen on ABA modified glassy carbon rotating disk electrode(O_2 saturated 0.5M H_2SO_4, 10mV/s)

Knowing i_l it is possible to plot ln [$i_k / (i_k - i_l)$] vs the electrode potential E (Fig. 25.) gives a straight line with a slope 1/ b (15.79 dec / V) and an intercept at the origin - ln (i_l / i^o) is about -6.35. From these results a Tafel slope 63.3mV /dec and an exchange current density of 4.8×10^{-6} A/cm^2 were calculated. The limiting current density resulting from a mixed control (i_l) is much higher (by a factor of 5.7×10^2 times) that of the exchange current density i^o. This confirms that the electron transfer step is rate determining.

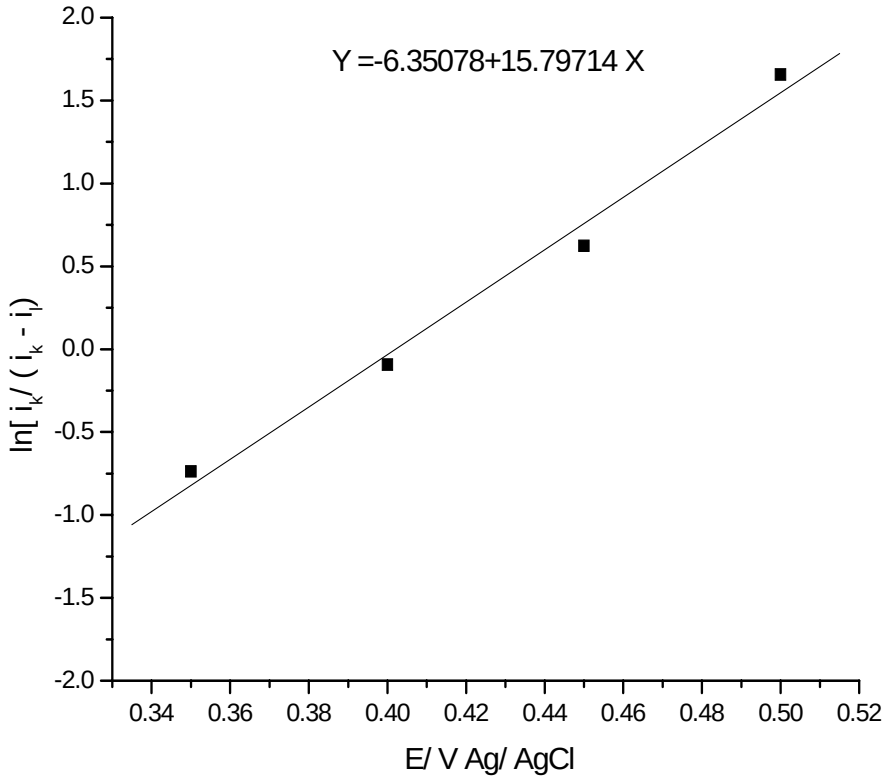

Fig. 25 Plot of ln[i_k/ (i_k - i_l)] vs E for the reduction of oxygen on ABA modified glassy carbon rotating disk electrode (O_2 saturated 0.5M H_2SO_4, 10mV/s)

6.3. Electrocatalytic reduction of oxygen on 8-aminonaphtalene-2-Sulfonic acid (ANSA)

6.3.1 Cyclic voltammetry

The reduction of oxygen dissolved in 0.5 M H_2SO_4 supporting electrolyte was investigated at GC/ANSA. The current vs potential curve (Fig. 26) were recorded during a slow voltammetric sweep (sweep rate 10mV/s)

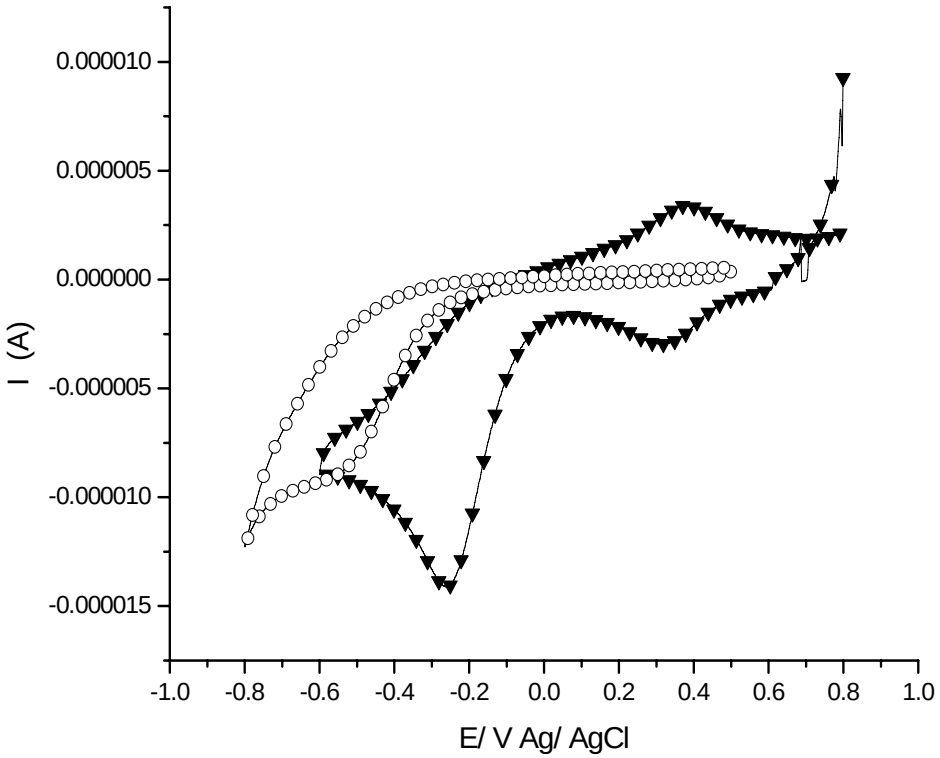

Fig. 26. CVs of: bare GC electrode in O_2 Saturated(O), and O_2 saturated GC/ANSA ▼ (O_2 saturated 0.5M H_2SO_4, 10mV/s)

In the presence of O_2 a new peak was developed at -257 mV. This cathodic peak corresponds to the electrochemical reduction of oxygen at the GC/ANSA electrode (Fig. 26 curve ▼).The electrochemical reduction of oxygen at a bare GC electrode shows a broad ill defined cathodic peak (curve O) and the cathodic peak potential is located at about -541mV.Based on the above results, it was concluded that GC/ANSA electrode reduced the overpotential required for O_2 reduction about 284mV.Furthermore, the peak currents of curve (O) is less than that in curve (▼).

All the above results indicated that the GC/ANSA electrode has electrocatalytic activity for the electrochemical reduction of O_2.

6.3. 2 Oxygen reduction reaction at ANSA modified rotating disk glassy Carbon Electrode

The reduction of oxygen dissolved in 0.5M H_2SO_4 supporting electrolyte was investigated at GC/ANSA rotating disk electrode for several rotation speeds ω (from 100 to 3200 rpm). The current vs potential curve (Fig. 27) were recorded during a slow voltammetric sweep (sweep rate $10mVs^{-1}$**).**

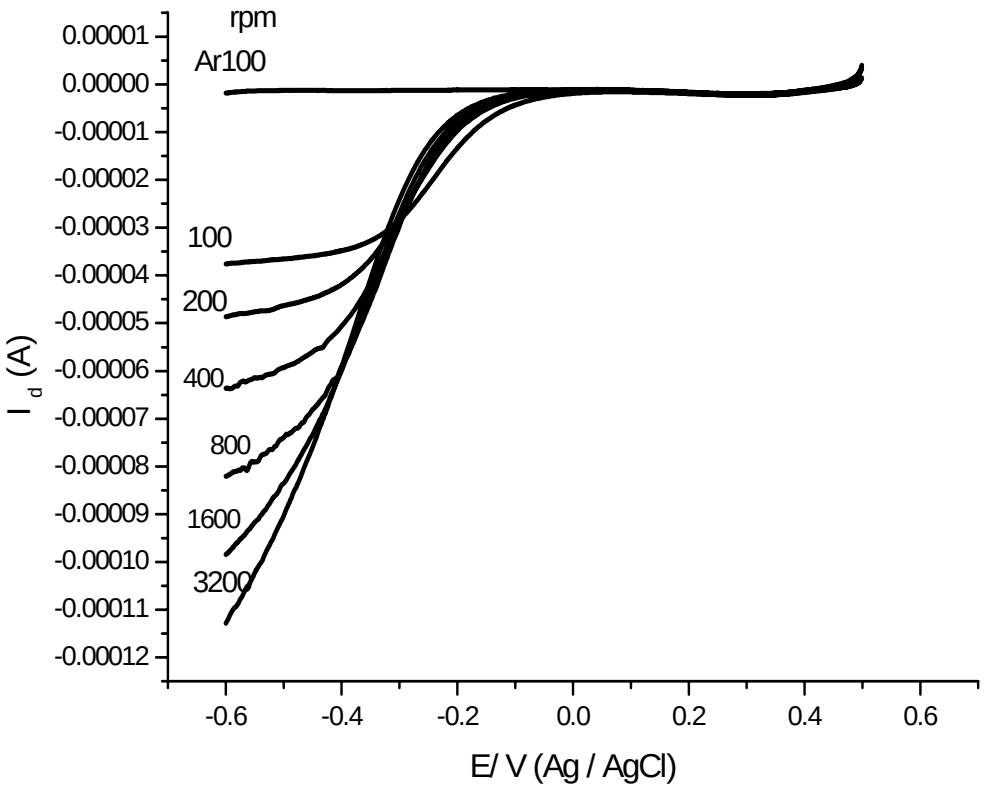

Fig. 27 Rotating disk voltamograms for reduction of oxygen (1.03mM) at ANSA /GC disk electrode for six different rotation speeds (O_2 saturated 0.5M H_2SO_4, 10mV/s)

In Fig. 27 the onset of oxygen reduction was observed at about -0.1 V Vs Ag/ AgCl and plateau region was observed. The limiting current was observed and increased with the rotation speed. A Levich plot (i_l vs $\omega^{1/2}$) for oxygen reduction reaction at ANSA modified glassy carbon electrode in an O_2 saturated 0.5M H_2SO_4 solution is shown in Fig. 28.

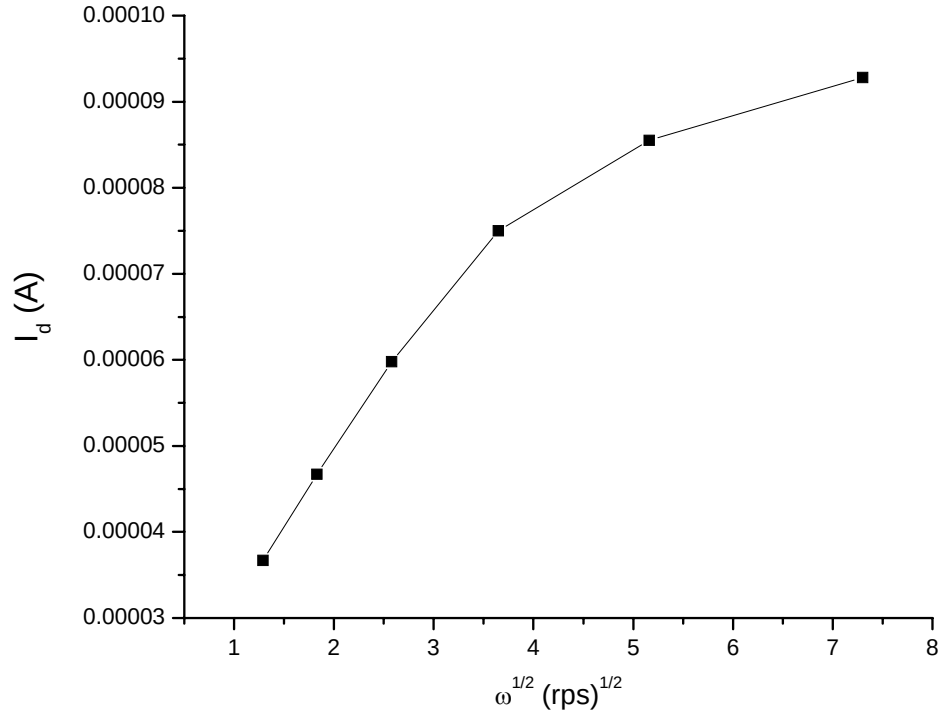

Fig. 28 Levich plot for the reduction of oxygen at ANSA modified glassy carbon electrode (O_2 saturated 0.5M H_2SO_4,10mV/s)

In Fig. 28 the Levich plot derived from the limiting current at a potential of -0.51 V is non linear for a reaction in which a current limiting chemical step precedes the electron transfer .The Koutecky-Levich plots (Fig. 29) is very close to the theoretical calculated line for a four electrons process (n=4) which indicates the accomplishment of the reduction of O_2 to H_2O.

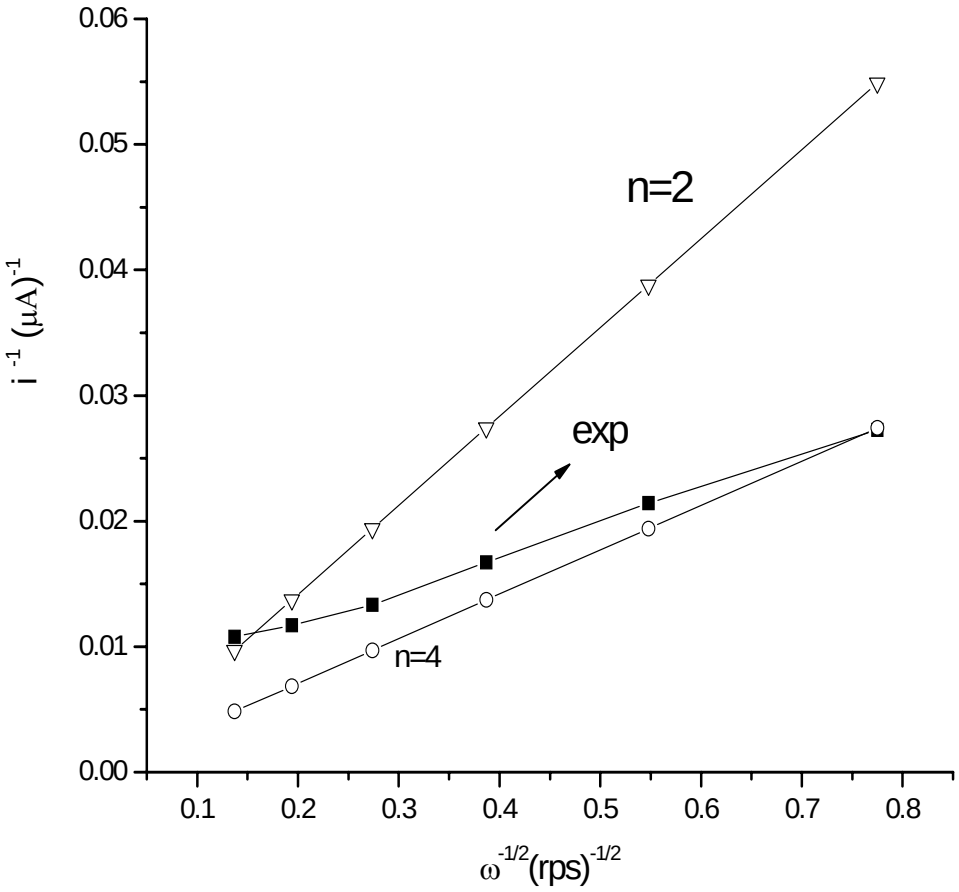

Fig. 29 Koutecky-Levich plots i^{-1} vs $\omega^{-1/2}$ for the reduction of oxygen on ANSA /GC rotating disk electrode (O_2 saturated 0.5M H_2SO_4, 10mV/s) for theoretical (2es and 4es) and experimental result.

As represented in Fig. 30 plots of i^{-1} vs $\omega^{-1/2}$ give good linearity. If the disk potential (ED) shifts from less negative (-0.45 V) to more negative (-0.57 V) the intercept of the i^{-1} vs $\omega^{-1/2}$ Curves becomes smaller. This indicates that the catalytic reaction moves from a kinetically controlled process to a mass transport controlled process.

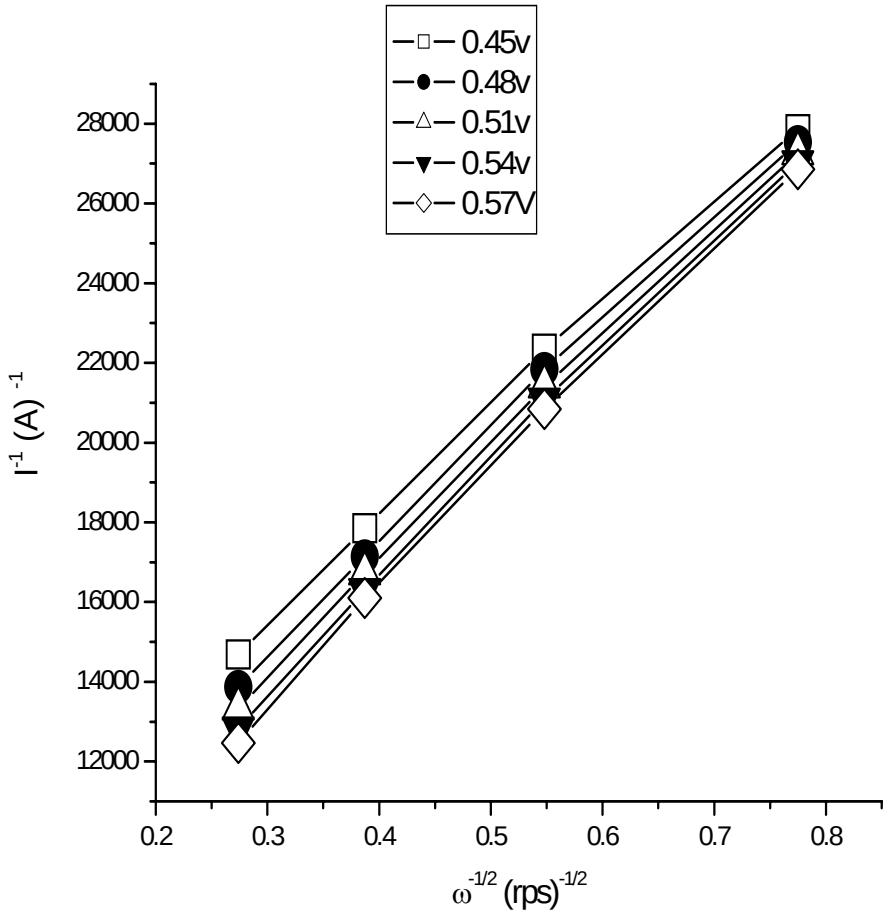

Fig. 30 Koutecky-Levich plots i^{-1} vs $\omega^{-1/2}$ for the reduction of oxygen on ANSA /GC rotating disk electrode (O_2 saturated 0.5M H_2SO_4, 10mV/s) at a different potential.

The kinetic contribution to the total current increases if the disk potential moves from less negative to more negative values (Fig. 31). As the potential become more negative it would be more favorable for electron transfer reaction.

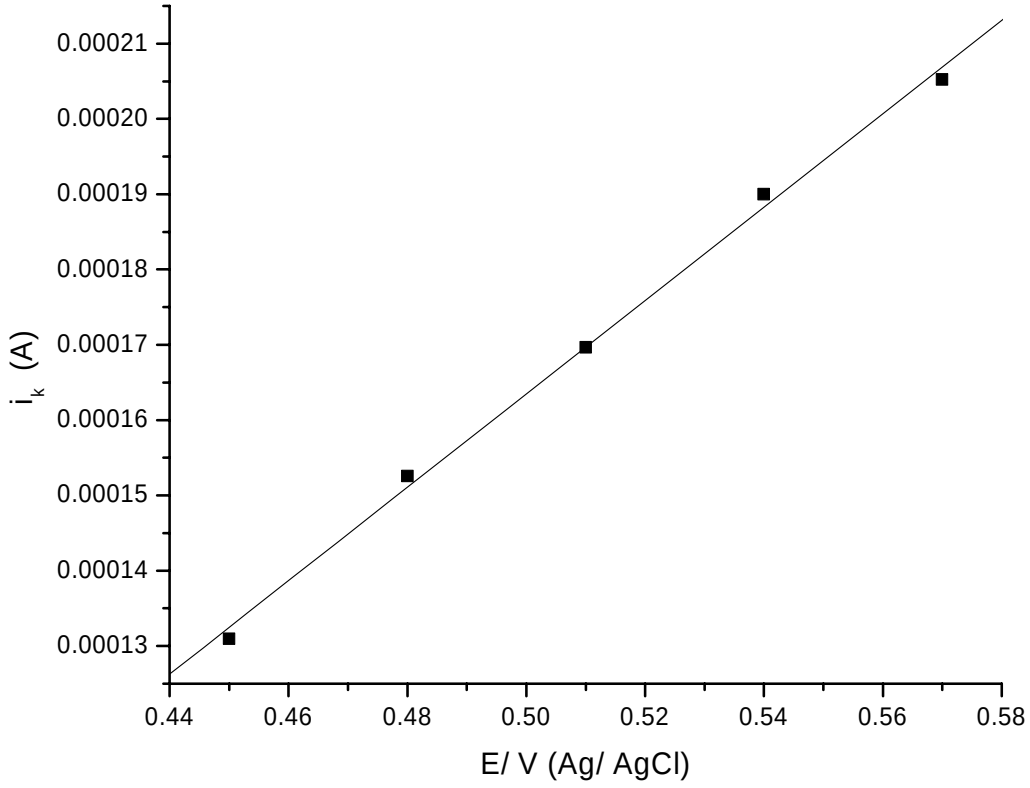

Fig. 31 Pot of i_k vs potential for the reduction of oxygen on ANSA/GC rotating disk electrode (O_2 saturated 0.5M H_2SO_4, 10mV/s) at a different potential.

Plot of $1/ i_k$ vs the electrode potential (E) Fig. 32 allows to determine the limiting current density resulting from a mixed control (i_l) obtained by extrapolating eq. (34) at high η. The value of $1/i_l$ obtained was 345.18 cm^2A^{-1} and i_l was found to be 2.9×10^{-3} A/cm^2.

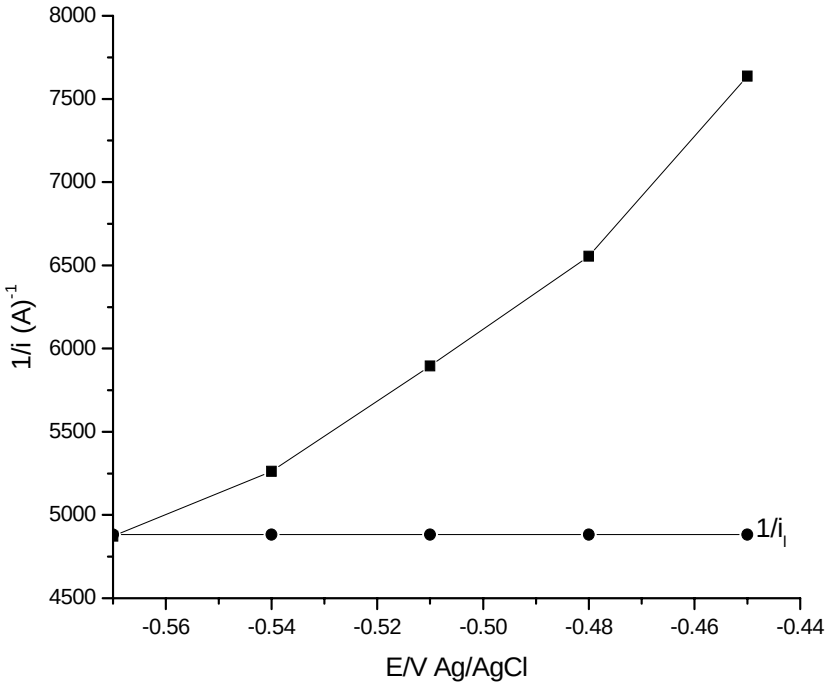

Fig. 32 Plot of $1/ i_k$ vs the electrode potential for the reduction of oxygen on ANSA modified glassy carbon rotating disk electrode (O_2 saturated 0.5M H_2SO_4, 10mV/s)

Knowing i_l it is possible to plot ln [$i_k / (i_k - i_l)$] vs the electrode potential E (Fig. 33) gives a straight line with a slope 1/ b (16.68 dec / V) and an intercept at the origin - ln (i_l / i^o) is equal to -6.394. From these results a Tafel slope 60mV /dec and an exchange current density of 2.8 $x10^{-6}$ A/cm^2 were calculated. The limiting current density resulting from a mixed control (i_l) is much higher (by a factor of 10^3 times) that of the exchange current density i^o. This confirms that the electron transfer step is rate determining.

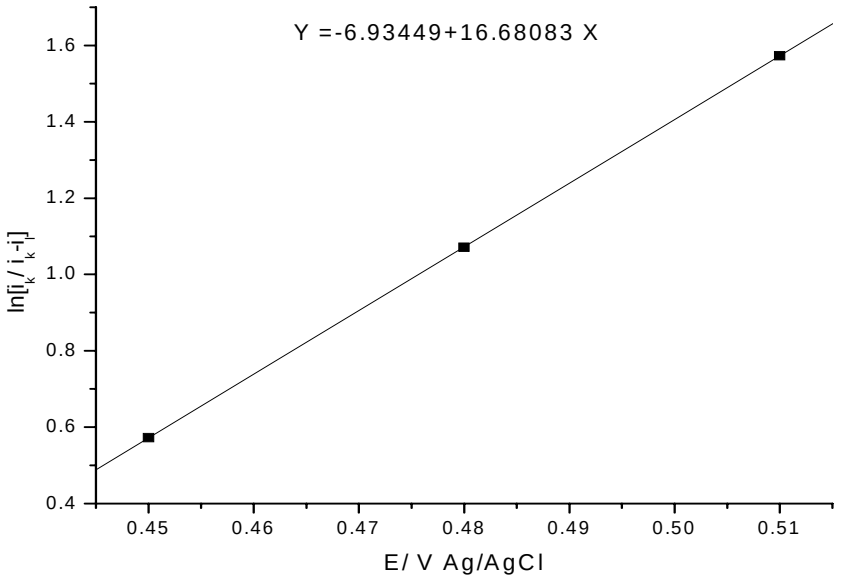

Fig. 33 Plot $\ln[i_k/ (i_k - i_l)]$ vs E for the reduction of oxygen on ANSA modified glassy carbon rotating disk electrode (O_2 saturated 0.5M H_2SO_4, 10mV/s)

Table 2

Kinetic parameter for oxygen reduction reaction on different polymer modified glassy carbon electrodes

GC modified with	Limiting current density i_l (A/cm^2)	Tafel slope (b) mV/dec	Exchange current density i^o(A/cm^2)	Overpotential (η) for 1.0A/cm^2 current density
AHNSA	5.9×10^{-3}	79.21	1.7×10^{-6}	457 mV
ABA	2.744×10^{-3}	63.3	4.8×10^{-6}	336 mV
ANSA	2.9×10^{-3}	60	2.8×10^{-6}	325 mV

Usually, the exchange current density (i^o) values are used to measure the electrocatalysis of substances. One disadvantage of the i^o comparison standard is that it neglect the influence of the Tafel slope. If one is interested in practical or engineering aspects of catalysis, the comparison should be made in the range of current in which the device is destinated to operate. In this case the value of the Tafel slope can be as important as i^o in determining the overpotential at current density of practical interest [33]. The trend in overpotential in Table 2. is in agreement with the data obtained (Table 3) from cyclic voltammetry for the three polymer modified electrodes.

The largest peak current from CV data were obtained for 4-amino-3-hydroxynaphtalene sulfonic acid (AHNSA) modified glassy carbon electrode which is attributed to the highest limiting current density resulting from adsorption step.

Table 3
Comparison of overpotential for oxygen reduction reaction on different polymer modified glassy carbon electrodes

Electrode	Bare GC	GC/ AHNSA	GC/ ABA	GC/ ANSA
Ep of ORR (mV)	-541	-340	-272	-257
The decrease in η compared to GC(mV)		200	269	284

7. CONCLUSIONS

The analysis of electrochemical behavior and the electrocatalytic activity of polymer modified electrode can be examined using cyclic voltammetric and rotating disk voltammetric techniques.

The analysis of kinetic data recorded for ORR at 4-amino-3-hydroxynaphtalene sulfonic acid (AHNSA), 2-aminobenzoic acid (ABA) and 8-aminonaphtalene-2-sulfonic acid (ANSA) modified glassy carbon electrodes, led to the following important conclusions.

- In all the three polymer modified glassy carbon electrodes the limiting current density resulting from a mixed control (i_l) is much higher than that of the exchange current i^o. This implies that the oxygen reduction reaction is not controlled by the adsorption step.

- 4-amino-3-hydroxynaphtalene sulfonic acid (AHNSA) modified glassy carbon electrode having the highest i_l is the best in allowing the species to move in the film and has the fastest adsorption step of all the three polymer modified glassy carbon electrodes.

- 2-aminobenzoic acid (ABA) modified glassy carbon electrode having the highest exchange current density (i^o) is the best electrocatalyst for ORR.

- 8-aminonaphtalene -2- sulfonic acid (ANSA) modified glassy carbon electrode having the minimum overpotential is the best electrocatalyst from engineering aspect for ORR.

8. REFERENCES

[1]. S.A. Kumar, S. Chen, J. Mol. Catal. A: Chem. 278 (2007) 244.

[2]. H. Park, T. Kwon, D. Park, Y. Shim, Bull. Korean Chem. Soc. 27 (2006) 1763.

[3]. F. Scholz, Electroanalytical Methods: Guides to Experiments and Application, 1st ed., Springer, Berlin, 2002, p. 29.

[4]. P. Manisankar, A. Gomathi, Electroanalysis 17 (2005) 1051.

[5]. J. Lipkowski and P.N. Ross, Electrocatalysis, Wiley-VCH, New York, 1998.

[6]. E.D. Jeong, M.S. Won, and Y. Shim, Bull. Korean chem. Soc. 19 (1998) 417.

[7]. J. Hwang and J.S. Chung, Electrochim. Acta 38 (1993) 2715.

[8]. H. Yang, W. Vogel, C. Lamy, and N. Alonso, J. Phys. Chem. B: 108 (2004) 11024.

[9]. V. Jalan and E.J. Taylor, J. Electrochem. Soc. 130 (1983) 2299.

[10]. S. Mukerjee and S. Srinivasan, J. Electroanal. Chem. 357 (1993) 201.

[11]. M.K. Min, J. Cho, K. Cho, and H. Kim, Electrochim. Acta 45 (2000) 4211.

[12]. M.T. Paffet, G.J. Beery, S.J. Gottesfeld, J. Electrochem. Soc. 142 (1995) 1531.

[13]. Q. Deyang, Carbon, 45 (2007) 1296.

[14]. N. Alonso, H.Tributsch, and O. Solorza-Feria, Electrochim. Acta 40 (1995) 567.

[15]. J.O'M. Bockris and U.M. Shared, Surface Electrochemistry, plenum, New York, 1993.

[16]. J. Ulstrup, J. Electroanal. Chem. 79 (1977) 191.

[17]. F. Beck, J. Appl. Electrochem. 7 (1977) 239.

[18]. M. Winter and R.J. Brodd, Chem. Rev, 104 (2004) 4245.

[19]. Z. Yang, G. Hu, Y. Liu, J. Zhao, G. Zhao, Canadian J. Anal. Scien. and Spectro. 52 (2006) 11.

[20]. T. Kissinger, and R. Heineman, Laboratory Techiniques in Electroanalytic Chemistry, 2nd ed., Marcel Dekker, New York, 1996, p. 315.

[21]. M. Mohammad, E. Payam, N. Hossein, M. Bibifatemeh, Turk J. Chem. 32 (2008) 571.

[22]. A. Malinauskas, Synth. Met. 107 (1999) 75.

[23]. J. O'M. Bockris and A.K.N. Reddy, Modern Electrochemistry 2B: Electrodics in Chemistry, Engineering, Biology and Material science, 2nd ed., Plenum, New York, 2000, p. 1612-1614.

[24]. R.A. Durst, A.J. Baumner, R.W. Murray, R.P. Buck, C.P. Andrieux, Pure Appl. Chem. 69 (1997) 1317.

[25]. V.G. Khomenko, V.Z. Barsukov, A.S. Katashinskii, Electrochim. Acta 50 (2005) 1675.

[26]. A.J. Bard, L.R. Faulkner, Electrochemical Methods: Fundamentals and Applications, 2nd ed., John Wiley and sons, New York, 2000.

[27]. J. Wang, Analytical electrochemistry, 3rd ed., John Wiley and sons, New York, 2006.

[28]. V.B. Vesovic, N.A. Anastasijevic, and R.R. Adzic, J. Electroanal. Chem. 218 (1987) 53.

[29]. M.J. Croissant, W.T. Napporn, J.M. Leger, C. Lamy, Electrochim. Acta 43 (1998) 2447.

[30]. J. Koryta, J. Dvorak, and L. Kavan, Principles of Electrochemistry, 2nd ed., John Willey and sons, New York, 1987, p. 319.

[31]. B.C. Kappl, Instrumental Method in Electrochemistry, Harwood publishing Chichester, England, 2004, 357-365.

[32]. M.J. Croissant, W.T. Napporn, J.M. Leger, C. Lamy, Electrochim. Acta 46 (2000) 579.

[33]. E. Gileadi, Electrode kinetics for Chemist, Chemical Engineers, and Material Scientist, Wiley-VCH, New York, 1993.